# THE UNIVERSITY OF HULL


## The impact of galaxy orientation on neighbour galaxy counts

Thesis submitted for the MSc (by Research) Physics

in the University of Hull

by

**Afrida Alam, MPhys Physics (University of Leicester)**

August 2021

# Acknowledgements

I would like to express my gratitude to my supervisor Dr Kevin Pimbblet for guiding me in this academic journey and for all his support and patience. I would also like to extend my gratitude to Dr Yjan Gordon for all his invaluable advice and suggestions. I want to thank Prof. Brad Gibson and the rest of the Physics department for fostering such a welcoming and enriching academic environment at the University of Hull.

Finally, I want to thank my parents and my sister for their love and support.

# Declaration of Originality

This thesis is submitted for the degree of MSc by Research from the University of Hull and was carried out under the supervision of Dr Kevin Pimbblet. This work is original and my own, except where otherwise stated and referenced.

Afrida Alam

August 2021

# Abstract

We utilised data from Galaxy Zoo, Sloan Digital Sky Survey and Yang et al. (2007) catalogue to determine if a galaxy's orientation, i.e. whether it is viewed edge-on or face-on, impacts the number of observed neighbour galaxies. The results showed that there is an excess of neighbours for edge-on galaxies than for face-on galaxies, once parameters such as halo mass and average stellar mass were controlled. For edge-on galaxies, the mean count and median of neighbours were 31.78 and 16.00, with lower and upper quartiles of 5.00 and 40.00. For face-on galaxies, the mean count and median were 12.88 and 10.00, with lower and upper quartiles of 6.00 and 16.00. This indicates that this an observational bias rather than a physical effect and face-on galaxies obscure their neighbours leading to fewer detections.

This result could have consequences for the unified theory of active galactic nuclei (AGN) which states that the difference between Type 1 and Type 2 AGN is a line-of-sight effect relative to an observer and their environments should not differ. However, studies have observed an excess of neighbours around Type 2 AGN compared to Type 1 AGN. We conducted a preliminary test to determine whether this excess is observed when separating the sample by Type 1 and Type 2. The results showed that for Type 1 AGN, the mean count and median of neighbours were 30.91 and 18.00 for edge-on galaxies, and 12.64 and 10.00 for face-on galaxies. For Type 2 AGN, the mean count and median were 24.50 and 10.00 for edge-on galaxies, and 12.25 and 8.50 for face-on galaxies. Therefore, there is an excess of neighbours for edge-on galaxies than for face-on galaxies in both Type 1 and Type 2 AGN. Future works could look at whether we could attribute this excess to edge-on galaxies being more likely to be associated with Type 2 AGN.

# Contents

# List of Figures

# 1. Introduction

## 1.1 Cosmological Models

Observations have revealed that the mass and energy density of the Universe is composed of approximately 5% ordinary, luminous (or baryonic) matter, 25% dark matter, and 70% dark energy (Planck Collaboration et al., 2016; Hinshaw et al., 2013). The first evidence for dark matter was observed in the Coma galaxy cluster where the velocities of the galaxies were higher than the expected values given their total mass (Zwicky, 1933). The origin and behaviour of dark energy is not fully understood despite its abundance, but it is assumed to be responsible for the accelerating expansion of the Universe as observed in distant supernova (Schmidt et al., 1998; Riess et al., 1998; Perlmutter et al., 1999).

The Lambda Cold Dark Matter ($\Lambda$CDM) model, the cold dark matter model with Einstein's cosmological constant $\Lambda$, has become the standard cosmological model in recent years (Blumenthal et al., 1984; Davis et al., 1985; Lahav et al., 1991), where $\Lambda$ is the energy density of space which is introduced as a result of Einstein's field equations of general relativity. According to this model, dark matter is cold because the particles became non-relativistic during the early stages of the formation of the Universe, and as a result could only travel negligible or small distances. These particles only interact with gravitation and the weak nuclear force, and is referred to as dark matter because of their lack of interaction with electromagnetic radiation. According to the $\Lambda$CDM model, dark matter comprises most of the mass content of the Universe and therefore dominates gravitationally on large scales. Hence, dark matter is crucial to the formation and evolution of galaxies and large-scale structures (see Figure 1.1 for a diagram showing the large-scale structure of the Universe).

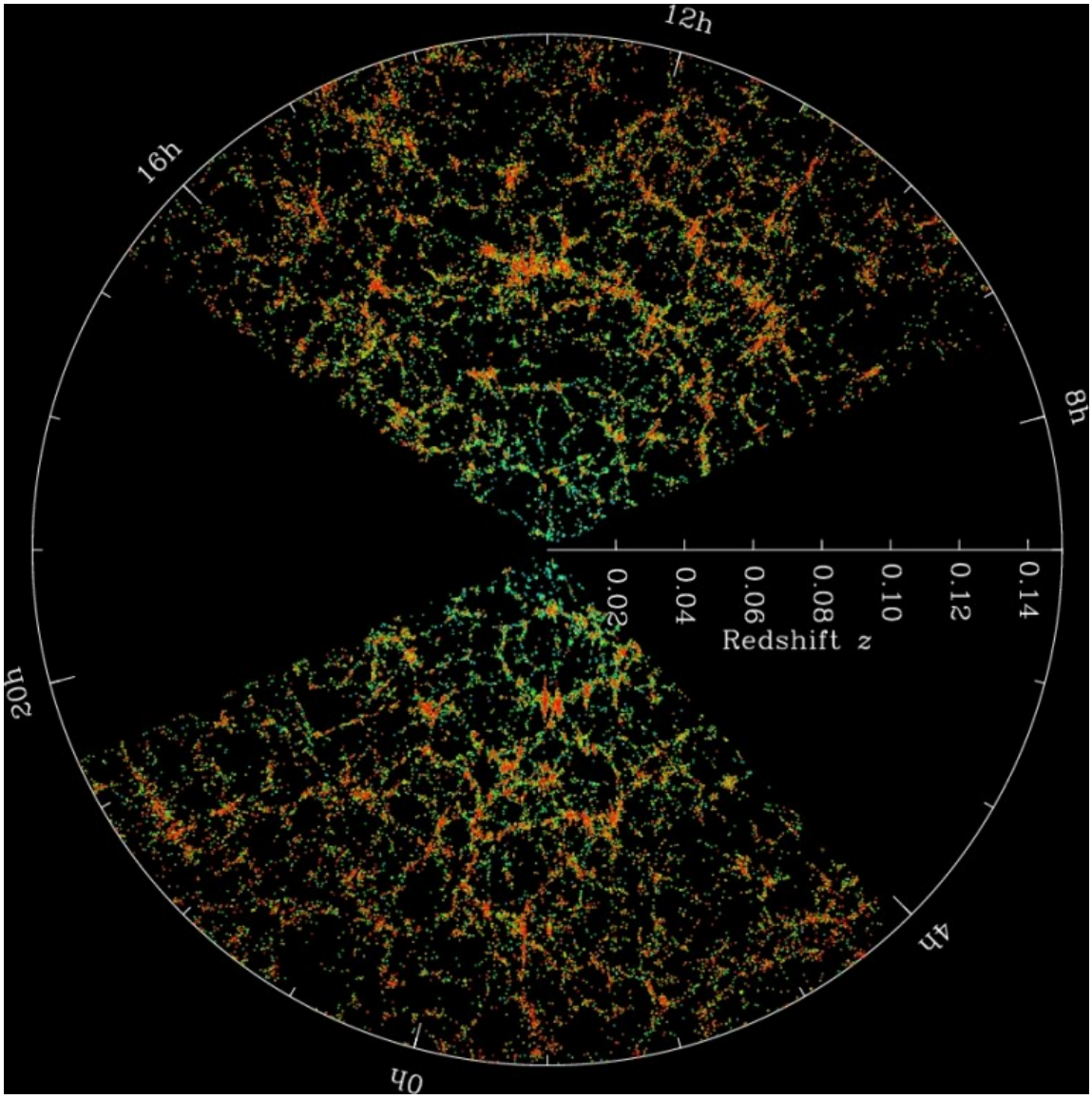


**Figure 1.1:** A diagram showing the large-scale structure of the Universe based on observations by Sloan Digital Sky Survey, where the galaxies or groups of galaxies are represented by a dot with older and larger galaxies corresponding to how red the dot is. Earth is at the centre of the figure and as such, a larger distance from Earth is indicated by a higher value of redshift. Therefore, this figure plots the sky coordinates of galaxies versus their distance away from Earth. Image credit: Sloan Digital Sky Survey, obtained from https://www.sdss.org/science

According to observations from WMAP (Hinshaw et al., 2013) and Planck Collaboration et al. (2016) the Universe started around 13.8 billion years ago and was in a hot, dense state and was mostly homogeneous. However, a rapid period of inflation amplified quantum fluctuations in the matter distribution, which created small inhomogeneities. These inhomogeneities can be detected through the temperature fluctuations in the leftover electromagnetic radiation from the early Universe, and this is referred to as Cosmic Microwave Background (CMB) radiation (Penzias & Wilson, 1965; Peebles, 1965; Gawiser & Silk, 2000). As the Universe expanded, these fluctuations and inhomogeneities grew and caused some regions to become over-dense and collapse due to self-gravity, and form dark matter halos (Peebles, 1980). Hence, these dark matter halos can be regarded as regions of gravitationally bound matter which have decoupled from the expansion of the Universe and collapsed onto itself.

The ΛCDM model shows that these dark matter halos grew hierarchically where small dark matter halos formed initially and then merged with each other to become bigger halos (White & Rees, 1978; Navarro et al., 1996). Baryonic, that is to say visible, matter was gravitationally attracted to these halos, and formed gaseous clouds. The gas cooled and collapsed to form cold and dense disks at the centre of the halos where they eventually collapsed further and formed the first galaxies (Zel'Dovich, 1970; Lacey & Cole, 1994).

Further collapse was able to ignite and sustain star-formation in these galaxies since dense regions form stars as per solar nebular theory (Woolfson, 1993), and feedback from this star-formation influenced galactic evolution and the surrounding environment. In addition to star-formation rate and supernovae feedback, the latter of which is the process whereby mass is ejected from the galaxy because of a supernova which inhibits the star-formation rate, a galaxy can undergo a number of other processes after its formation that will determine its properties and characteristics. Such processes include accretion of gas onto galaxies, ram pressure stripping (Toomre & Toomre, 1972), harassment (Moore et al.,

1996), and galaxy mergers (Pearson et al., 2019).

Different galactic environments provide different mechanisms which act upon a galaxy on different time-frames and mass-scales throughout its evolution. During the early dense stages of the Universe, galaxies gravitationally attracted one another and formed pairs, groups, or clusters and influenced each other in their evolution. An example of this is hierarchical merging, where smaller galaxies merge to form larger structures (Cole et al., 2000).

## 1.2 Galactic Environment and Evolution

### 1.2.1 Galaxy Morphology

The morphological classifications of galaxies are important since observations reveal that different types of galaxies are more abundant in different environments (Dressler, 1980). Therefore, classification schemes, such as morphological classification, can be used to gain insights on galaxy formation and evolution. Galaxies were first classified according to their morphologies by Edwin Hubble (Hubble, 1926) and were done "by eye" which lead to some missing classes and uncertainty when compared to the current classifications. The Hubble sequence splits galaxies broadly into three major categories: elliptical, spiral, and lenticular (Figure 1.2) with an additional fourth group called irregular (Conselice, 2014).

Elliptical galaxies have an ellipsoidal or spheroid shape and are typically smooth systems with no distinguishable internal structures. These galaxies mainly consists of a bulge with zero disk and have varying ellipticities. As such, elliptical galaxies are labelled as E$n$ where $n$ is an integer representing the galaxy's ellipticity and ranges between 0 and 7, with 0 representing a circular galaxy and 7 being a galaxy that is flatter and thinner.

Spiral galaxies consist of a disk and a bulge with spiral arms extending from the latter and are divided into two groups: S and SB. S spiral galaxies or unbarred spirals have arms which extend from the central bulge, whereas SB galaxies or barred spirals have arms

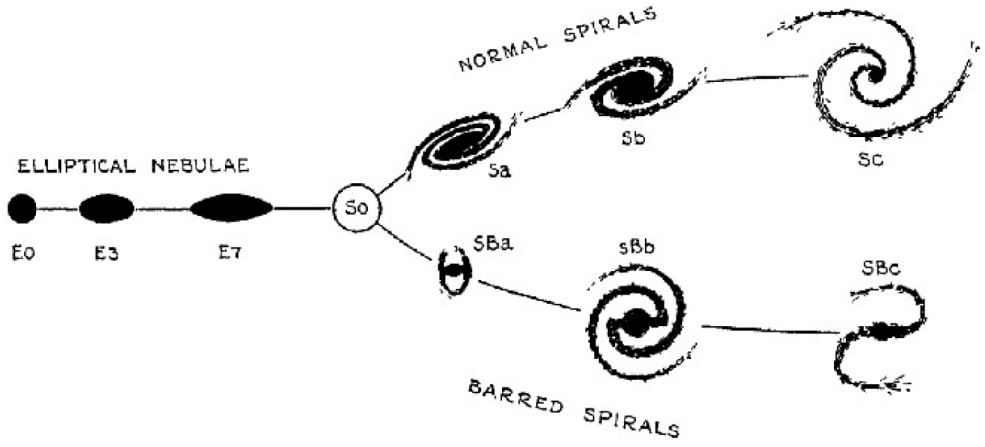


**Figure 1.2:** Diagram of the Hubble Sequence (Hubble, 1926) where the left-hand side shows elliptical galaxies and the right-hand side is composed of spiral galaxies (both barred and unbarred), and the two are joined in the middle by lenticular galaxies. It was mistakenly thought that the diagram represented an evolutionary sequence where galaxies progressed from left to right. As a result, elliptical galaxies were called early-type and spiral galaxies were called late-type. Even though this is incorrect and was not stated by Hubble, the terminology early-type and late-type are still used to refer to elliptical and spiral galaxies respectively.

which extend from the central bar-shaped structure. These two groups of S and SB can be further divided into smaller groups of a, b, and c and this classification depends on how open or tightly coiled the spiral arms are.

Lenticular (or S0) galaxies have similarities with both elliptical and spiral galaxies and in the Hubble sequence they are found between the two, and are speculated to represent a transitional phase from elliptical to spiral galaxies. Irregular (or Irr) galaxies are galaxies with irregular or abnormal shapes and do not exhibit any spiral or elliptical symmetries. These galaxies are formed by violent events and are usually regarded as a separate group from the previous three.

Galaxy morphological features such as ellipticities, bars and arms can provide crucial

insights into the mechanisms and processes that influenced its evolution. For example, a central bulge in a disk galaxy can indicate past galactic mergers (Martig et al., 2012; Conselice, 2014), whereas the presence of bars can indicate slow secular evolution (Kormendy, 2013). The correlation between the morphology of a galaxy and the density of the environment in which it resides is referred to as the morphology-density relation (Figure 1.3). The morphology-density relation is confirmed by observations which show that elliptical and lenticular galaxies are more prevalent in higher density regions than spiral and irregular galaxies (Dressler, 1980; Postman & Geller, 1984). This relation implies that other critical properties, such as star formation and the mechanisms driving them, may also correlate with the properties of the host environment.

### 1.2.2 Galaxy Luminosity Function

A galaxy's formation and growth is expected to be coupled to the growth of its host halo in the current paradigm. This means that properties, such as its luminosity or the total mass of its stellar components should be connected to halo properties such as the halo mass. The halo mass function is defined as the number density of halos at a given mass and can be determined by theoretical models (White, 2001). Subsequently they can be compared to the luminosity function of galaxies, where we can consider a galaxy's luminosity to be the sum of its individual stellar luminosities. Since the mass-luminosity function states that a star's luminosity and mass are related (Eddington, 1924), we can infer a galaxy's total stellar mass from its luminosity. However, this comparison reveals a discrepancy between the galaxy's luminosity or stellar mass function and the halo mass function at the high and low mass ends (Figure 1.4; Mutch et al., 2013).

The discrepancy suggests that at these points there exists some mechanism(s) which regulates and inhibit the stellar mass growth and as a result limits the stellar mass or luminosity functions. At the low mass end, this could be due to stellar feedback such

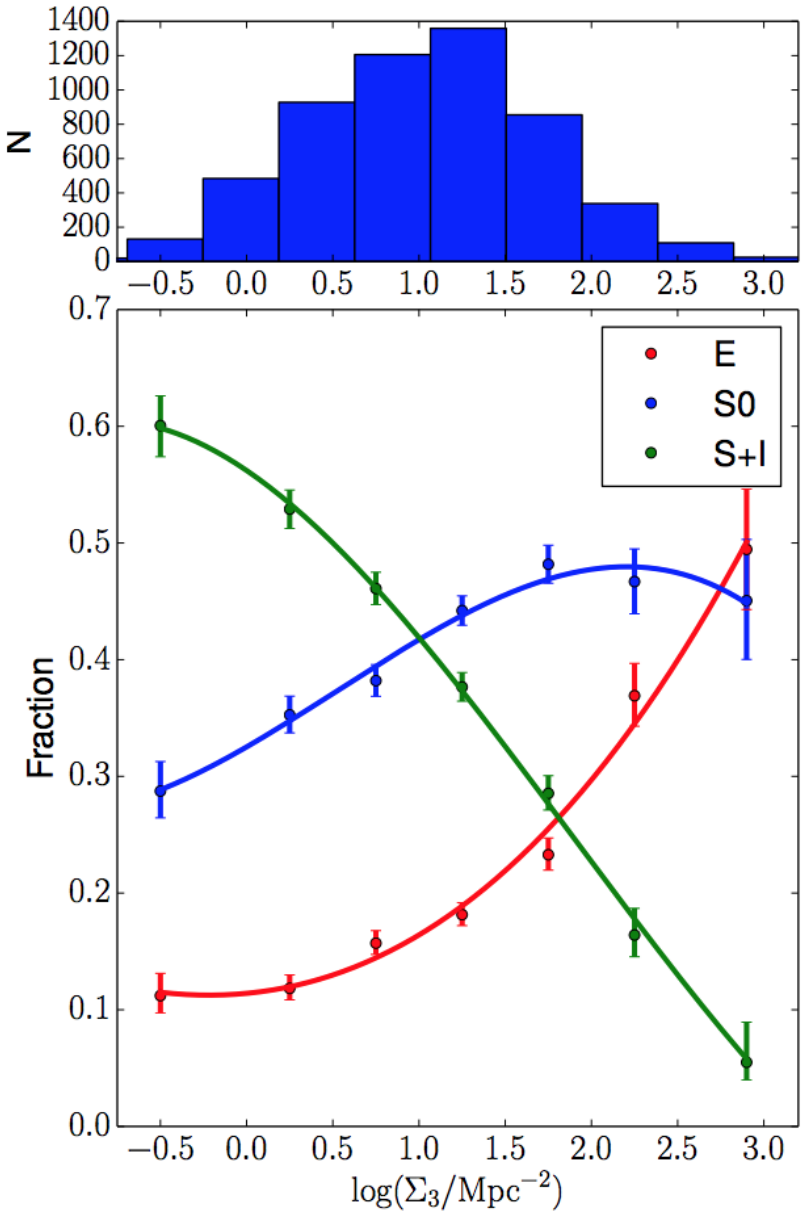


**Figure 1.3:** Diagram from Houghton (2015) which shows the morphology-density relation where the fraction of elliptical (E), lenticular (S0), spiral and irregular (S+I) galaxies are given per density bin and the density $\Sigma_3$ is given by the projected density to the third nearest neighbour.

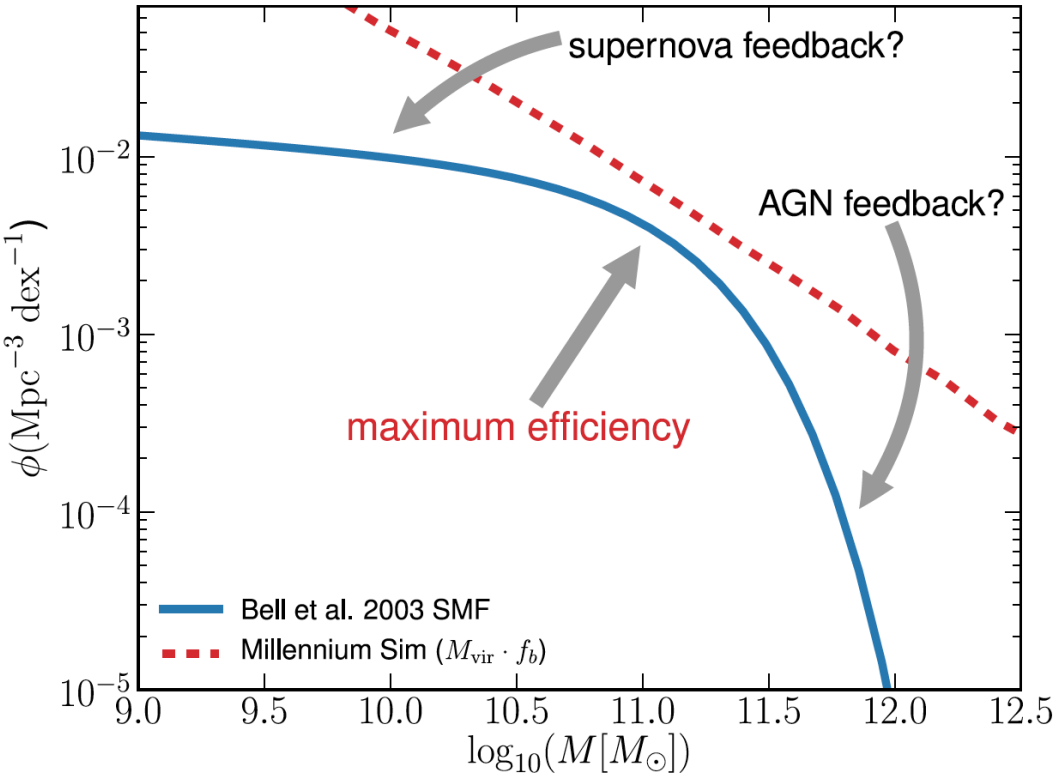


**Figure 1.4:** Diagram from Mutch et al. (2013) showing the comparison between the stellar mass function (blue curve; Bell et al., 2003) to the halo mass function (red dashed line; Springel et al., 2005). There is a discrepancy between the two functions at the high and low mass ends of the stellar mass function and this can be attributed to AGN and supernovae feedback respectively. These mechanisms inhibit stellar mass growth and is theorised to cause the discrepancy between the two mass functions.

as supernovae feedback (Scannapieco et al., 2008) which removes the fuel required for star-formation. At the high mass end, the discrepancy is theorised to be because of active galactic nuclei (AGN) where the accretion of matter onto the black holes lead to energy release that heat the surrounding gas or remove it from the galaxy through processes such as radio jets and winds (Croton et al., 2006; Fabian, 2012).

### 1.2.3 Galaxy Colour

In addition to a galaxy's morphology, another key visual property is its colour. Galaxy colour is defined as the difference in magnitudes between two different photometric bands, for example B-V where B is the magnitude as measured in the B-band and V is measured in the V-band. Since passbands are measured logarithmically, colours can be considered to be the ratio of red to blue light. This property is important because it is closely related to components such as the stars, gas, and dust that reside within the galaxy. For example, if galactic colours and their absolute magnitudes are plotted against each other in a colour-magnitude diagram, it shows that the galaxies can be divided into two groups: one with bluer colours and the other which is redder (Figure 1.5). Based on the Hertzsprung-Russell diagram (Russell, 1914), it can be inferred that galaxies in the red sequence have little star-formation and are likely to consist of more redder and older stars. Galaxies in the blue cloud will have more active star-formation and consist of more younger and bluer stars. The gap between these red and blue regions is a transitional region called the 'green valley'.

It has been noted that a galaxy's morphology is closely tied to its colour, where galaxies in the red sequence in the colour-magnitude diagram generally tend to be early-type galaxies such E or S0. On the other hand, galaxies in the blue cloud are typically late-type such as S/SB & Irr (Strateva et al., 2001; Schawinski et al., 2014). As a result, it can be inferred that most elliptical galaxies have not undergone any recent star-formation and are mainly composed of an older stellar population.

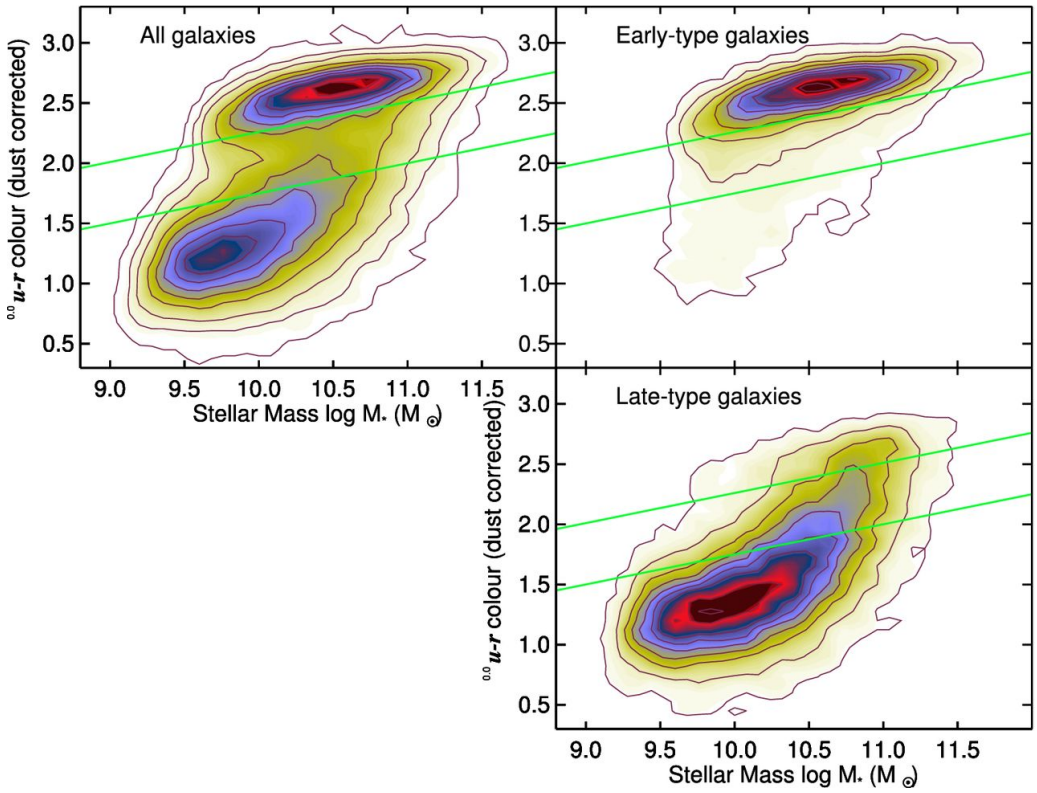


**Figure 1.5:** Colour-mass diagram from Schawinski et al. (2014) (with formative works carried out by Visvanathan & Sandage, 1977 and Bower et al., 1998 in this topic) which shows the bimodal distribution of the galaxies in terms of colour and absolute stellar mass. The top left graph shows all the galaxies in the sample and the separated early-type and late-type galaxies are shown in the right. The 'All galaxies' diagram shows that there are two peaks, where the peak at the top corresponds to galaxies in the red sequence (higher values of $u - r$) and the second peak at the bottom corresponds to galaxies in the blue cloud (lower values of $u - r$). The transitional green valley region between these two peaks is marked by the green lines.

They contain little dust or gas and are considered to have formed through galaxy mergers between two or more galaxies of similar mass (De Lucia et al., 2006). Conversely, spiral galaxies are usually actively star-forming and thus have bluer colours. These galaxies contain significant dust and gas and their emission lines tend to dominate the galaxy's spectrum. However, there are rare types of galaxies which go against these trends, such as red spirals which have lower star-formation rates than blue spirals in all environments, which indicates a lack of an explicit correlation between the star-formation rates of red spirals and its environment (Masters et al., 2010).

### 1.2.4 Central and Neighbour Galaxies

The properties of the host dark matter halo influence the evolution of a galaxy and its environment. Galaxies are generally observed in groups residing in a single dark matter halo as a result of hierarchical merging (Cole et al., 2000), where groups of 100 galaxies or more are referred to as clusters (Abell, 1958).

In such a dark matter halo, the dominant galaxy, which tends to be near the centre of the halo and is generally the most luminous and massive galaxy, is referred to as the central galaxy (Skibba, 2009; Lange et al., 2017). The surrounding galaxies which orbits this central galaxy are subsequently referred to as its neighbour or satellite galaxies and are usually bluer and fainter than the central galaxy (Weinmann et al., 2009). This indicates that central and neighbour galaxies are at different stages of evolution or that the processes driving their evolution might be different. For example, the process driving the evolution of central galaxies is thought to be strongly linked to AGN feedback processes such as jets and winds which inhibits or 'quenches' star-formation (Croton et al., 2006; Fabian, 2012). However, for neighbour galaxies, star-formation is thought to be inhibited by processes such as harassment by other neighbour galaxies, ram pressure stripping, and strangulation. The latter, which is the process in which the hot gas reservoirs of the neighbours have

been stripped, is considered to be the most likely mechanism (Van Den Bosch et al., 2008). Moreover, it has been found that the quenching of star-formation in neighbour galaxies is strongly correlated to its distance to the centre of the group, that is to say that star-formation rates in denser environments are quenched more effectively and this can also be seen in clusters (Woo et al., 2016; Wang et al., 2018).

## 1.3 Overview of Black Holes and AGN

It is well accepted that most, if not all, massive galaxies contain a SMBH at its centre (Kormendy & Ho, 2013). In such galaxies, the SMBH accretes matter and the gravitational potential of the infalling matter is converted into radiative energy. The accretion process in a radiatively-efficient system creates a disk of accreting material called an accretion disk. An AGN is defined as a galaxy which contains an accreting black hole with mass $> 10^5 M_\odot$ and Eddington ratio exceeding the limit of $L_{\rm AGN}/L_{\rm Edd} = 10^{-5}$ at its centre (King & Pounds, 2015), and the term central engine is used to refer to the SMBH and accretion flow in an AGN.

AGN were first identified from the emission lines in their optical spectra (Seyfert, 1943). They can be categorised based on observational properties such as their luminosity, spectrum and the ratio of the central engine's luminosity to that of the host galaxy. Seyfert galaxies are galaxies which are classed as an AGN based on spectral line properties, where early observations of Seyferts were biased towards lower luminosity AGN in early-type spiral galaxies. Quasi-stellar objects (QSOs or quasars) are characterised as more luminous versions of Seyfert galaxies with similar spectra but they are usually found in greater distances than Seyferts. LINERs (low-ionization nuclear emission-line regions) are an additional AGN class which fall below the Seyferts on the luminosity scale, though not all LINERs are expected to be low luminosity AGN as the line ratios can be caused by factors such as an ageing stellar population (Belfiore et al., 2016).

In addition, AGN can be classified in terms of their energy output: radiative-mode and jet-mode. The majority of the energy output in a radiative-mode AGN is in the form of electromagnetic radiation which spans across all wavelengths and results from matter being accreted through a geometrically-thin and optically-thick accretion disk situated within a few Schwarzschild radii of the SMBH. This group includes Seyfert galaxies and QSOs, and is generally found in young growing galaxies (Ho, 2008). On the other hand, jet-mode AGN are typically found in relatively older galaxies and are associated with more massive black holes. Gas in these galaxies is hot and there is relatively little star-formation occurring. The AGN accretion process in this scenario is inefficient, with the accretion rate being significantly below the Eddington limit (Heckman & Best, 2014).

Since only a small percentage of galaxies, roughly 10%, host an AGN (Martini et al., 2006) it raises the question of how and why such AGN are triggered. It is theorised that physical mechanisms that destabilise the cold gas reservoirs that already exist within a galaxy, such as harassment or ram pressure stripping, may create the right conditions for AGN triggering. This is because the galaxy harassment process can gravitationally perturb the gas within the galaxy or tidal interactions from such harassment can create tidal debris, which can then act as a fuel source for AGN triggering (Moore et al., 1996). Moreover, ram pressure stripping removes the outer gas from a galaxy and destabilises it and can trigger an infall of gas toward the centre of the galaxy, where it can be accreted by the SMBH and trigger an AGN (Tonnesen & Bryan, 2009).

## 1.4 AGN and Galaxy Evolution

There are strong correlations between the observed properties of the SMBH within an AGN and those of their host galaxies, especially that of the galactic bulge. Observations indicate a connection between the mass of the SMBH, $M$, and the velocity dispersion, $\sigma$, of the galactic bulge which is known as the $M-\sigma$ relation (Figure 1.6; Ferrarese & Merritt, 2000;

Gebhardt et al., 2000). In elliptical galaxies, the velocity dispersion of the galactic bulge is also related to the luminosity of the bulge ($L_{\rm bulge}$) by the Faber-Jackson relation which states that $L_{\rm bulge} \propto \sigma^4_{\rm bulge}$ (Faber & Jackson, 1976). Additionally, observations also show that the SMBH mass correlates tightly with the mass of the galactic bulge, $M_{\rm bulge}$, and this is referred to as the Magorrian relation (Figure 1.7), and is of the form $M \sim 10^{-3} M_{\rm bulge}$ (Magorrian et al., 1998; Merritt & Ferrarese, 2001). These relations suggest that the presence of the SMBH affects the large-scale structure and properties of the host galaxy's bulge and that the two co-evolve.

However, given that the SMBH mass constitutes a small fraction of the total bulge mass, the former's gravitational radius of influence is considerably weaker than that of the latter. As a result, the observed correlations stated above cannot be due to the gravitational influence of the SMBH alone. Therefore, there must also be alternative processes through which the SMBH affects the galactic bulge, for example through outflows and feedback mechanisms (King & Pounds, 2015). Furthermore, the effect of the AGN can extend to outside the host galaxy since such jets can have lengths on the scale of a few Mpc and thus can affect the surrounding environment (Blandford et al., 2019).

## 1.5 Scope of Thesis

As outlined in the literature review, the properties of a galaxy are strongly correlated with its environment, including the host dark matter halo mass. This correlation can be analysed by looking at galaxies residing in comparable halo masses and investigating their number of neighbour galaxies. However, it is important to take into consideration any potential biases that might arise when conducting environmental analysis using neighbour galaxies. In this thesis, we have addressed this issue by using data from Galaxy Zoo (GZ; https://data.galaxyzoo.org), Sloan Digital Sky Survey (SDSS; https://www.sdss.org) and Yang et al. (2007) catalogue in order to probe potential biases by testing to see if the

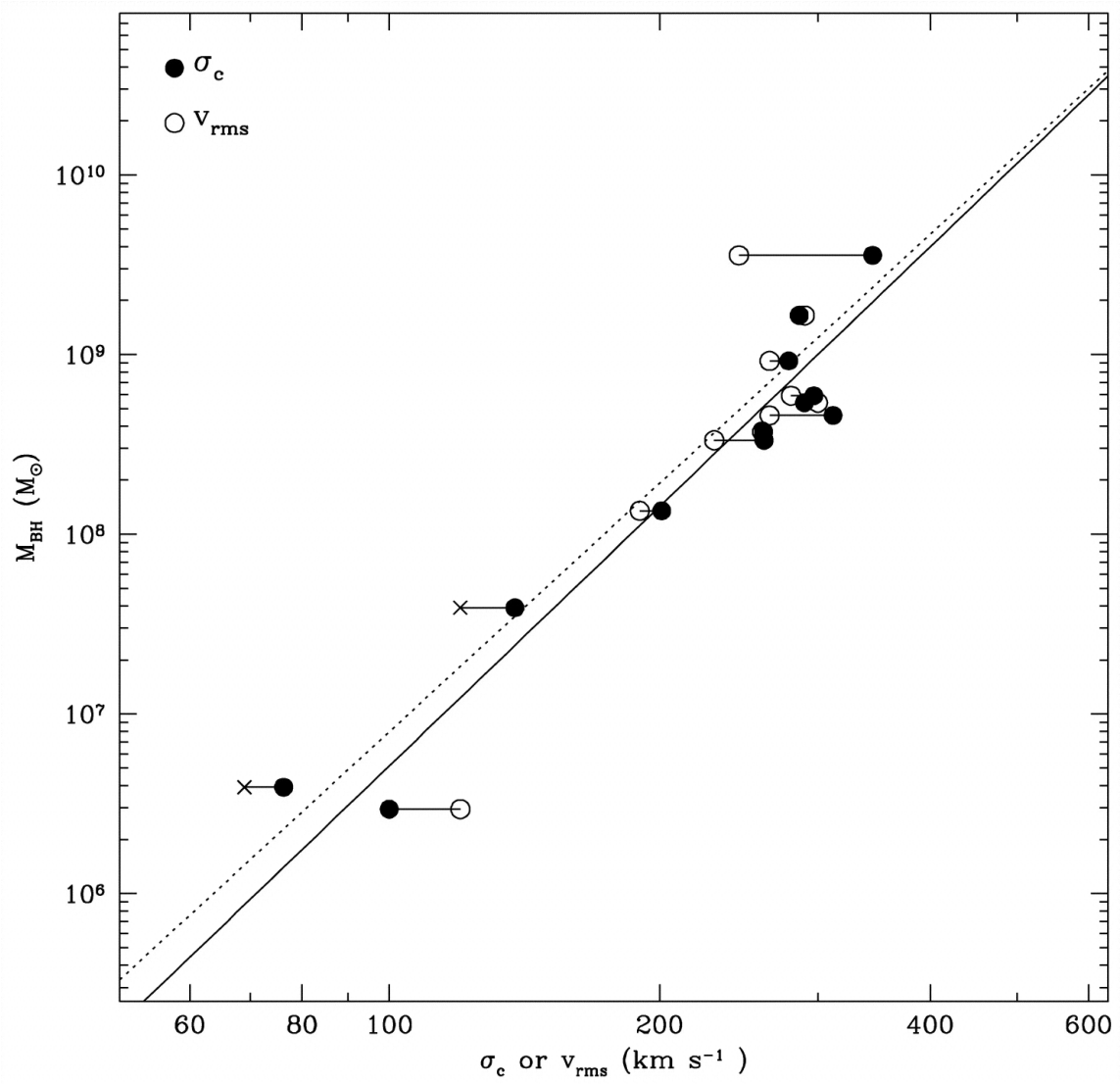


**Figure 1.6:** Graph from Ferrarese & Merritt (2000) which shows the strong correlation between the mass of the SMBH and the central velocity dispersion of the host galaxy's bulge (given by the solid circles). The solid line gives the best linear fit between the black hole mass and the velocity dispersion.

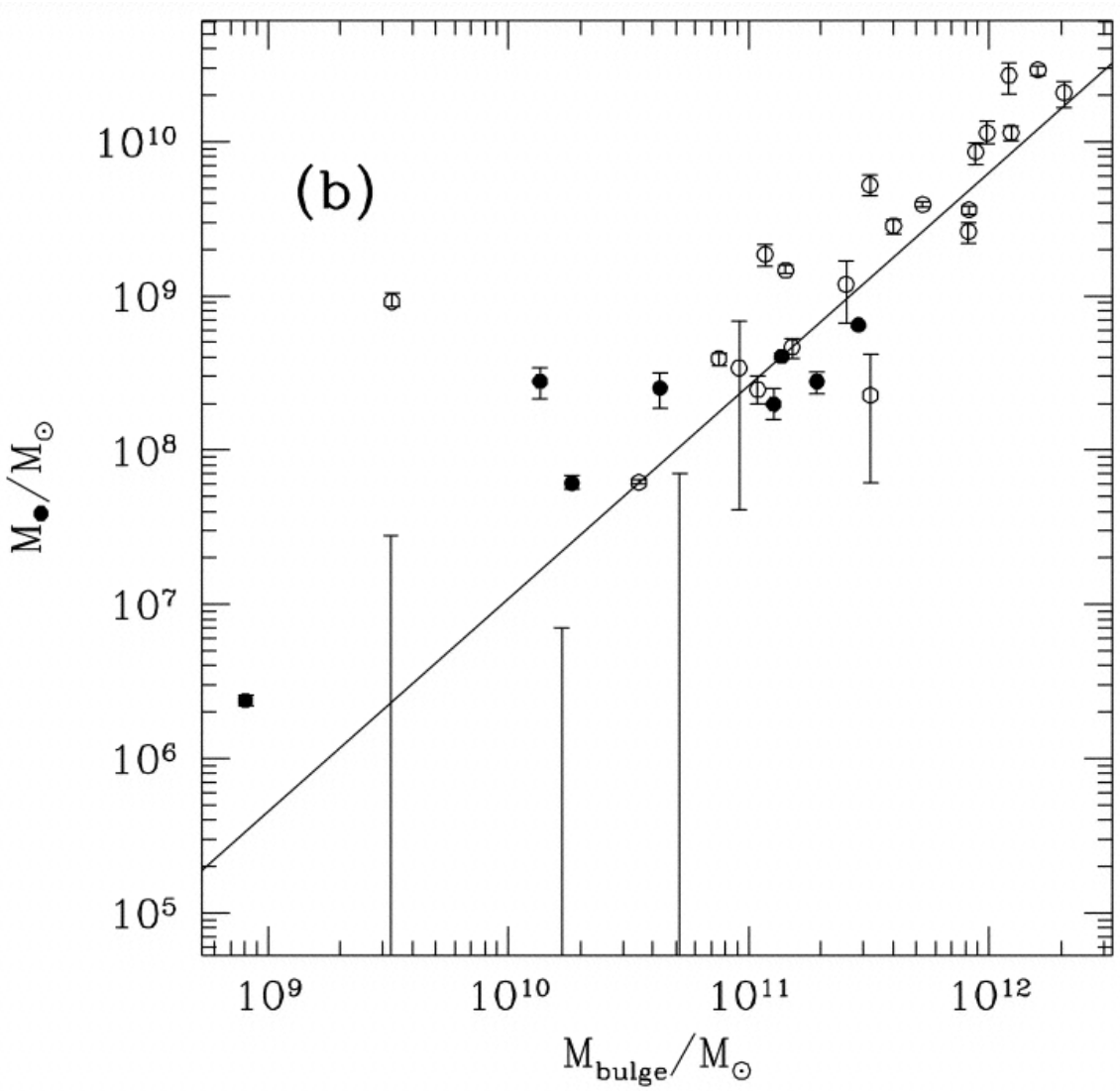


**Figure 1.7:** Graph from Magorrian et al. (1998) which shows a tight correlation between the SMBH mass (on the y-axis) and that of the central galactic bulge (on the x-axis), where the SMBH mass can be given approximately as a constant fraction of the galactic bulge mass.

orientation of a galaxy as observed impacted the number of neighbour galaxies that were detected. That is to say, we conducted tests to quantify if the number of neighbour galaxies observed differed between galaxies viewed edge-on than those viewed face-on.

Observations of excess neighbours could have consequences for the unified theory of AGN which states that Type 1 AGN (shows broad permitted and semi-forbidden emission lines) and Type 2 AGN (shows strong narrow emission lines in NIR-optical-UV wavelengths) are the same type of object and the differences between them arise from their orientation relative to an observer (Miller & Antonucci, 1983; Netzer, 2015; Hickox & Alexander, 2018). Therefore, the results of comparative environmental analysis of Type 1 and Type 2 AGN should reflect this. However, there has been an excess of neighbours observed around Type 2 AGN relative to Type 1 AGN (Dultzin-Hacyan et al., 1999; Koulouridis et al., 2006; Jiang et al., 2016; Villarroel & Korn, 2014; Gordon et al., 2016). Observations also show an excess of AGN in galaxies which exist in close pairs with other galaxies when compared to the number of AGN in the rest of the galactic population (Alonso et al., 2007; Ellison et al., 2011). Therefore, a potential future work would be to test if Type 2 AGN are more likely to be associated with edge-on galaxies than face-on and if this accounts for the excess of neighbours around Type 2 when compared to Type 1.

# 2. Data Selection

In this thesis, we used data from Sloan Digital Sky Survey (SDSS; https://www.sdss.org), Galaxy Zoo (GZ; https://data.galaxyzoo.org), and a halo mass catalogue developed by Yang et al. (2007).

## 2.1 Sloan Digital Sky Survey

The original Sloan Digital Sky Survey (SDSS) was an optical imaging and spectroscopic survey which mapped one quarter of the entire sky (with r < 17.77 across 9000 deg$^2$ for spectroscopy) and performed a redshift survey of stars, quasars, and galaxies (York et al., 2000). The data gathered in the survey contained photometric data across 5 broadband filters, $u, g, r, i, z$ with effective wavelengths of 3590 Å, 4810 Å, 6230 Å, 7640 Å and 9060 Å (Fukugita et al., 1996; Gunn et al., 1998), for more than 1.6 million objects. Additional photometry for deeper imaging was carried out on a stripe along the Celestial Equator in the Southern Galactic Cap (Stripe 82; Abazajian et al., 2009; Fliri & Trujillo, 2015). The default photometry available with the data release has an uncertainty of 1% in $g, r, i, z$, and 2% in $u$ (York et al., 2000).

Additional value-added data was also obtained from the MPA-JHU (Max Planck for Astrophysics and Johns Hopkins University) catalogue for SDSS Data Release 7 (DR7; Abazajian et al., 2009). This catalogue provided several derived properties based on SDSS spectra, including star-formation rates and stellar masses (Kauffmann et al., 2003; Salim et al., 2007; Brinchmann et al., 2004; Tremonti et al., 2004). The key values used in this thesis were stellar masses, which were calculated from fits to the photometry instead of stellar absorption features (Kauffmann et al., 2003; Salim et al., 2007).

An important caveat to note is that the SDSS spectroscopic sample suffers from incompleteness at small angular separations (< 55") because of fibre collisions. This is because the spectroscopic observations are carried out using fibre plug plates, and since each field has its own plug plate, it is not possible to spectroscopically observe both galaxies in a pair if they are separated by 55" (York et al., 2000). This can affect environmental studies using only spectroscopic samples, especially when investigating dense environments such as galaxy pairs or clusters (York et al., 2000; Yoon et al., 2008; Gordon et al., 2018).

## 2.2 Galaxy Zoo

We used data from the second data release of Galazy Zoo. Galaxy Zoo (GZ) is a citizen science project which recruits members of the public to classify images of galaxies online (Lintott et al., 2008; Lintott et al., 2010). The first version, GZ1, asked volunteers to classify around 1 million galaxy images as either smooth, spirals or mergers. In the second version, GZ2, volunteers were asked to make more detailed morphological classifications of over 300000 images from SDSS DR7 (which also included a subset of those which were already classified in GZ1; Willett et al., 2013).

Cuts were made to the dataset to ensure that the sample contained systems with clear morphological features that the participants could resolve and classify. Galaxies with a spectroscopic redshift outside the range $0.0005 < z < 0.25$ in the DR7 catalogue were removed in order to achieve this goal, although those without redshifts were kept. Once the data cuts were made, the main sample of images had a minimum of 16 classifications, a median of 44 and over 99.9% of the sample had at least 28 classifications. The final dataset contained 1634029 classifications made by over 80000 volunteers (Willett et al., 2013).

GZ2 volunteers made the classifications based on a decision tree that had 11 classification tasks with 37 possible responses in total (Figure 2.1). Willett et al. (2013) made

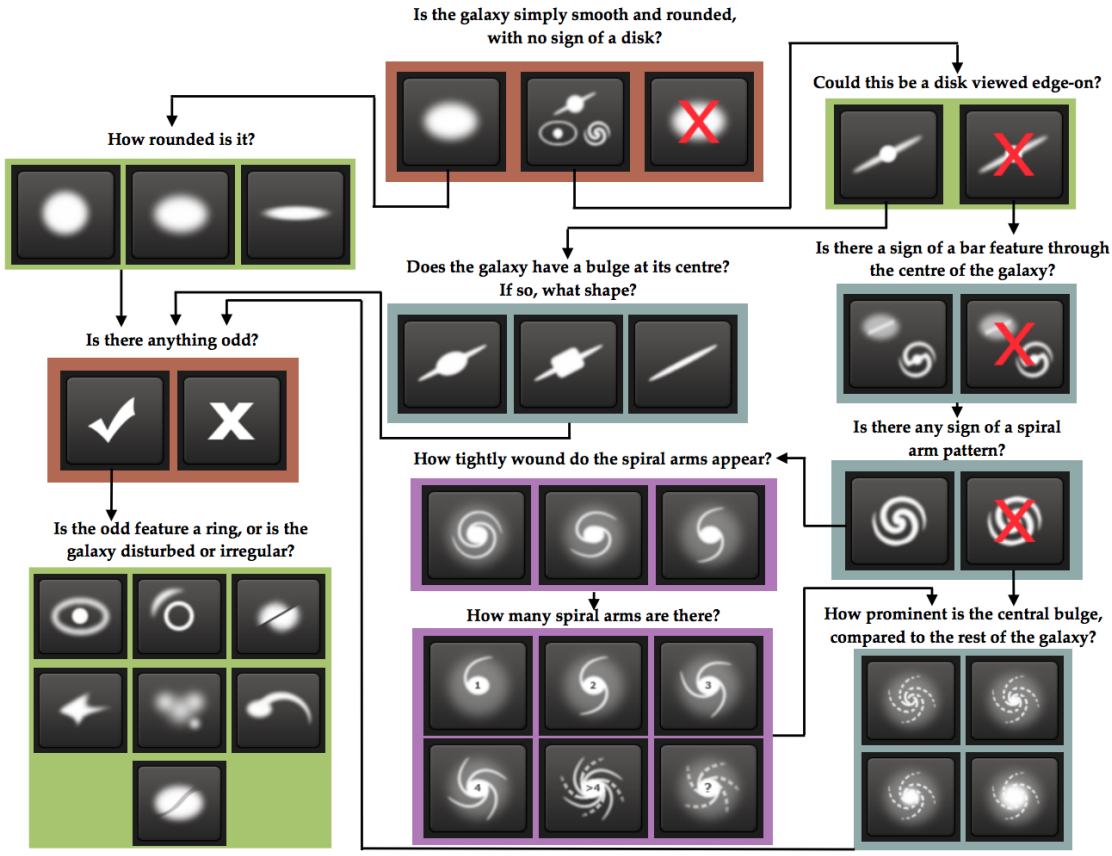


**Figure 2.1:** Galaxy Zoo decision tree from Willett et al. (2013). The first question (colour-coded in brown) was given to each participant. The second question on the right (colour-coded in green) which asked participants "Could this be a disk viewed edge-on?" was the key question focused on in this thesis.

adjustments to the vote fractions for classification bias following the same approach as Bamford et al. (2009). Since GZ2 had a decision tree, all questions after the first one depended on the answers given to prior questions. For example, in our case the question of whether a disk can be viewed as edge-on was only asked to participants if they previously answered that the galaxy in question had a disk. A threshold was set for the minimum weighted vote fraction for previous tasks and a minimum number of votes for a specific task in order to derive the bias correction for the task in question. Further details on debiasing for GZ2 can be found in Willett et al. (2013).

The data release included six parameters for each of the 37 morphological classes: the raw number of votes for a particular question, the number of votes weighted for a voter's consistency, the fraction of votes, the vote fraction weighted for consistency, the debiased likelihood and a Boolean flag (Willett et al., 2013). The Boolean flag was set if the galaxy was included in a debiased and clean sample which itself was determined by applying three criteria. The first criteria stated that the vote fraction for the prior questions must exceed a set threshold to ensure that the question was answered well. The second criteria stated that each question must exceed a minimum number of votes (20 for the main sample) as this reduced the impact of variance because of small number statistics. The third criteria stated that the debiased vote fraction must exceed a threshold of 0.80 for all questions. The three criteria taken together ensured that the GZ2 sample had the least bias possible.

## 2.3 Large Scale Structure Information

The data for dark matter halo masses were taken from galaxy group catalogues developed by Yang et al. (2007). They developed a halo-based group finder that is optimised for grouping galaxies residing in the same dark matter halo. This was done by initially identifying the centres of potential groups in order to make an estimation of the characteristic luminosity of each. The group finder used the average mass-to-light ratios and assigned an approximate

mass to each group by using an iterative approach. The mass was then used to estimate the host halo's velocity dispersion and size, and these were used to establish the members in the group redshift space. Subsequently, each group was assigned two values of halo masses based on either the characteristic luminosity $L_{19.5}$ (given by $M_L$) or the characteristic stellar mass $M_{stellar}$ (given by $M_S$) (Yang et al., 2007).

Applying the group finder to SDSS DR4 resulted in 301237 groups, and its performance was tested using comprehensive mock galaxy redshift surveys constructed from conditional luminosity function models. The performance test was conducted by taking into consideration the completeness of true members and contamination by potential interlopers, in addition to the accuracy of the assigned masses (Yang et al., 2007). The group finder was found to be more successful in grouping galaxies according to their common dark matter halos than the standard friends-of-friends (FOF) algorithm approach (which is a tool used to identify groups or clusters of points within a certain spatial distance) as the tests on the mock surveys showed that around 80% of all groups had a completeness of over 80% (Yang et al., 2007).

The group finder was subsequently used to construct group catalogues from the New York University Value-Added Galaxy Catalogue (Blanton et al., 2005), which is a collection of galaxy catalogues comprising samples of large-scale structures. The area covered by the photometric sample and the spectroscopic sample are 3514 $deg^2$ and 2627 $deg^2$ respectively, with completeness of about 85% (this does not include areas that bright stars have obscured). The key values used in this thesis were the halo mass and the photometric data in the $g$ and $i$ bands.

# 3. Methodology and Results

In this section, we outlined the method used to select and process the data described in Chapter 2. We subsequently analysed the data in order to identify the effect, if any, of galaxy orientation on neighbour satellite count.

## 3.1 Data Selection and Sample Generation

Using the data from SDSS, GZ2 and Yang et al. (2007) catalogue, we created subsets of edge-on and face-on galaxies. Given the three criteria for a galaxy to be flagged in GZ2 and included in a debiased and clean sample, we set the flag to equal to 1 for both edge-on and not edge-on (i.e. face-on) galaxies in order to ensure that the data being used was accurate and robust. The subsequent subsets had 1850 edge-on galaxies and 12047 face-on galaxies. Visual inspection of a small subset of randomly selected images (100 galaxies) showed that the data correlated with the classification and there were no false positives.

In order to generate a volume-limited and mass-limited sample, we imposed a redshift cut of $z < 0.05$ and the average stellar mass (the average of the probability distribution function of $\log M_*$ and is given in the AVG column) was limited to only include galaxies with mass values $> 10^{10} M_\odot$. These limits were found by determining the completeness of our sample, which is illustrated in Figure 3.1, and the completeness of the sample using these cuts is approximately 100%.

A sky crossmatch with SDSS DR7 was carried out using TOPCAT (Tool for OPerations on Catalogues And Tables) on the separate edge-on and face-on galaxy samples in order to find neighbour galaxies (given by the number of times a row has been duplicated) within a radius of up to 30 arcseconds. This yielded 14658 rows for edge-on galaxies and 125252

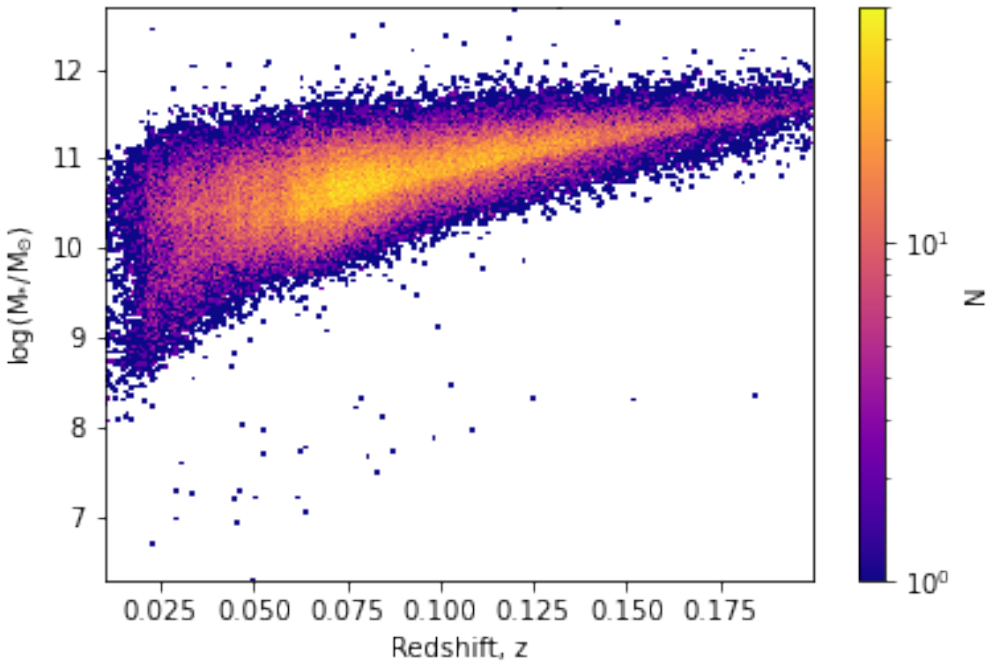


**Figure 3.1:** Density plot of redshift vs average stellar mass for the whole dataset of edge-on and face-on galaxies. At redshift $z = 0.05$ the completeness of the data is almost 100% for galaxies with average stellar mass down to $> 10^{10} M_{\odot}$.

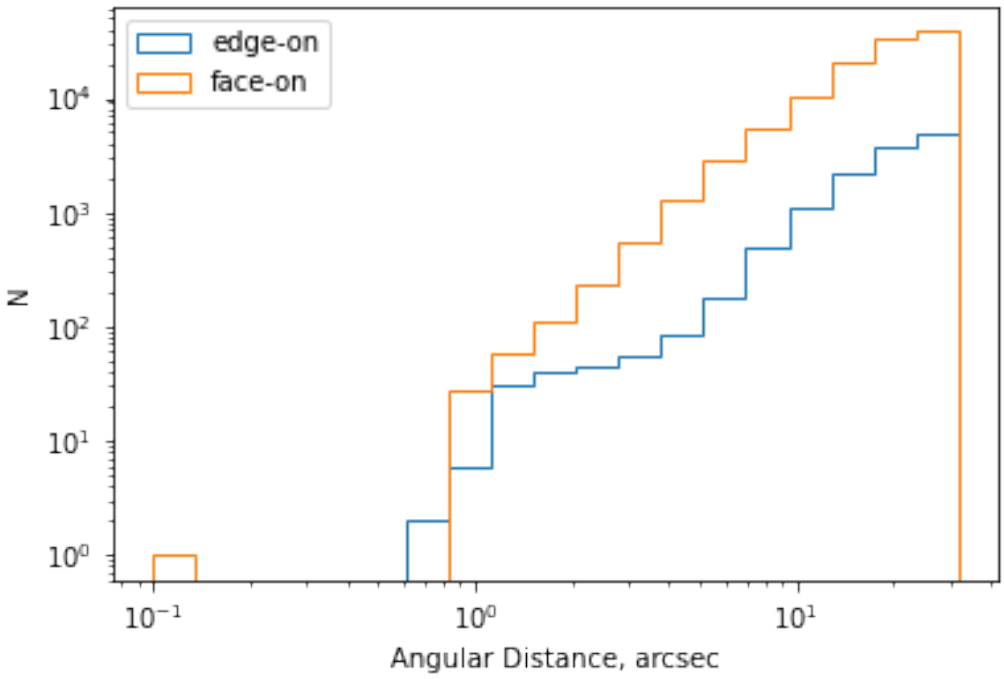


**Figure 3.2:** Plot of the angular distance or separation of the neighbours from the target galaxy for the whole dataset of edge-on and face-on galaxies. We set a minimum limit of the angular distance to 1.5 arcseconds in order to remove self-matches from the photometric catalogue.

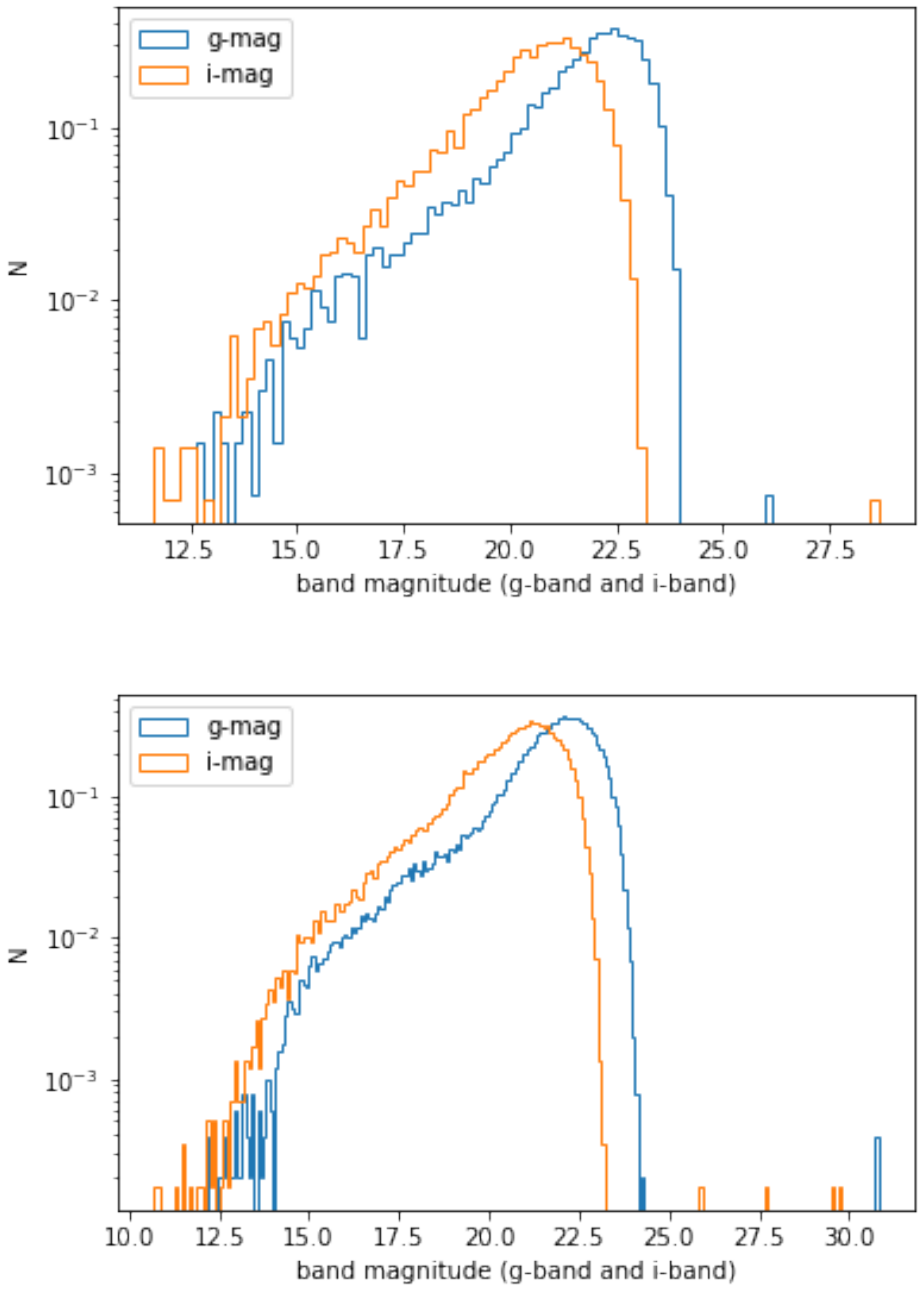


**Figure 3.3:** Distribution of magnitudes of the neighbour galaxies of edge-on (top figure) and face-on galaxies (bottom figure) in $g$ and $i$ bands with data from SDSS DR7. There is a 95% detection repeatability for point sources at 22.2 magnitude limit for $g$-mag and 21.3 for $i$-mag and we set these limits for the band magnitudes (Abazajian et al., 2009).

rows for face-on galaxies. A minimum angular separation from the target galaxy of 1.5 arcseconds was set to ensure that were no contamination of our sample of neighbours by the primary target galaxies themselves (Figure 3.2). The magnitude limit was set to $< 22.2$ for $g$-band and $< 21.3$ for $i$-band since there is a 95% detection repeatability for point sources at these limits (Abazajian et al., 2009), and completeness drops off after these values as seen when the magnitude of this dataset was plotted in Figure 3.3. These limits yielded 3937 rows for edge-on galaxies and 33071 rows for face-on galaxies.

## 3.2 Sample Control

In order to determine the role of orientation on neighbour counts, in this stage we controlled on the host halo mass, $M_{180}$, in the Yang et al. (2007) catalogue (which is the 10-based logarithm of the group mass in $h^{-1}$ $M_{\odot}$ and is given in the column Mgroup). We controlled the host halo mass since comparing edge-on galaxies in low mass halos and face-on galaxies in high mass halos would not be comparable since there would be fewer neighbours in smaller halo masses as established in Chapter 1. Additionally, we controlled for stellar mass such that the galaxies were in the same mass range so that the comparisons were reliable and fair.

Using the controls for halo mass and stellar mass, we matched face-on galaxies with edge-on galaxies of comparable halo mass and stellar mass to provide a robust control sample. We achieved this by creating a pool of face-on galaxies for each edge-on galaxy, as there were fewer edge-on galaxies compared to face-on in our dataset. These control pools contained face-on galaxies with halo masses and stellar masses within 0.25 dex (the errors in the halo masses varied between 0.20 dex and 0.35 dex; Yang et al., 2007; Gordon et al., 2019) and 0.10 dex (baseline tolerance for galaxy pairs established in Ellison et al., 2015) respectively of the edge-on galaxy. For each edge-on galaxy, a face-on galaxy was randomly selected from this subset so that they could be compared, and this yielded a

sample of 50557 neighbours for analysis.

From this sample, we plotted the halo mass (Figure 3.4) and average stellar mass (Figure 3.5) of the edge-on and face-on galaxies in the sample, as well as the magnitude of their neighbour galaxies in *g* and *i* bands (Figure 3.6), and the angular distance or separation of the neighbours from the edge-on and face-on galaxies (Figure 3.7) in order to see if the samples matched. As shown, the halo mass and average stellar mass of the edge-on and face-on galaxies in the sample were closely matched, and as was the magnitudes of the neighbours of edge-on and face-on galaxies in *g* and *i* bands, and the angular distance of the neighbours from the target galaxies.

## 3.3 Results and Discussion

Once a sample of edge-on galaxies with a corresponding face-on galaxy was generated, the count of neighbours observed for each was determined to see if there were any observational excesses or biases. The mean count and median was found to be 31.78 and 16.00 respectively for edge-on galaxies, and 12.88 and 10.00 for face-on galaxies. For edge-on galaxies, the lower quartile was 5.00 and the upper quartile was 40.00, while for face-on galaxies the lower quartile was 6.00 and the upper quartile was 16.00. The results show that there are more neighbour galaxies observed for edge-on galaxies than for face-on galaxies, and we plotted the distribution of the count in Figure 3.8. As established, the difference between edge-on and face-on galaxies is a line-of-sight effect given their orientation relative to an observer. Since we controlled for various key parameters such as halo mass and average stellar mass when creating the sample of edge-on galaxies and corresponding face-on galaxies, we would expect there to be a similar count of observed neighbours for both.

We have quantified the observational excess of neighbours around edge-on galaxies than face-on galaxies. We expect this difference in neighbour count to be an observational

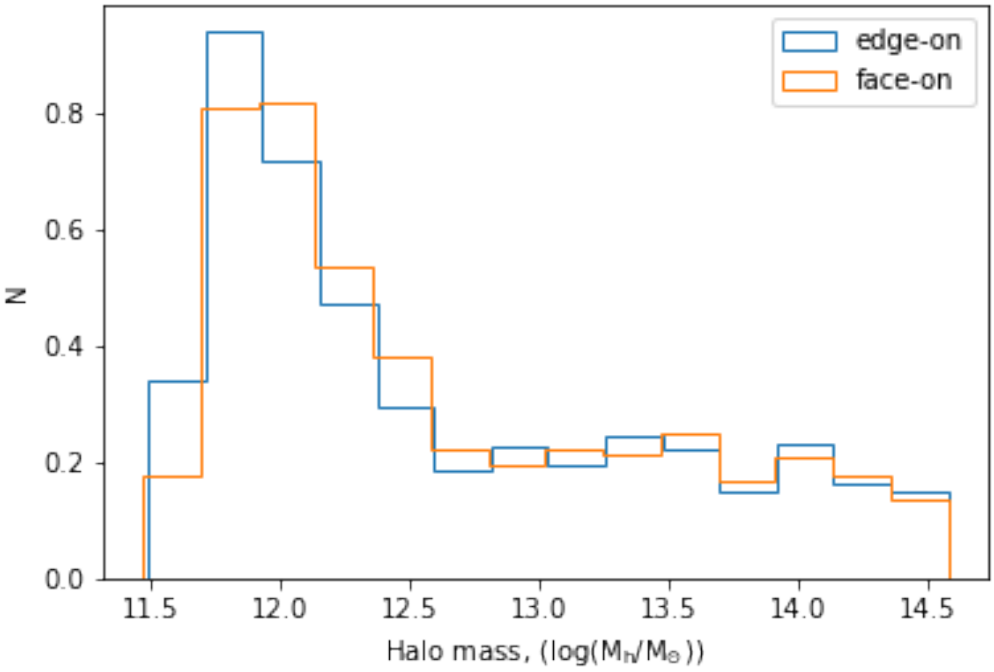


**Figure 3.4:** Halo mass of edge-on galaxies and face-on galaxies in the sample

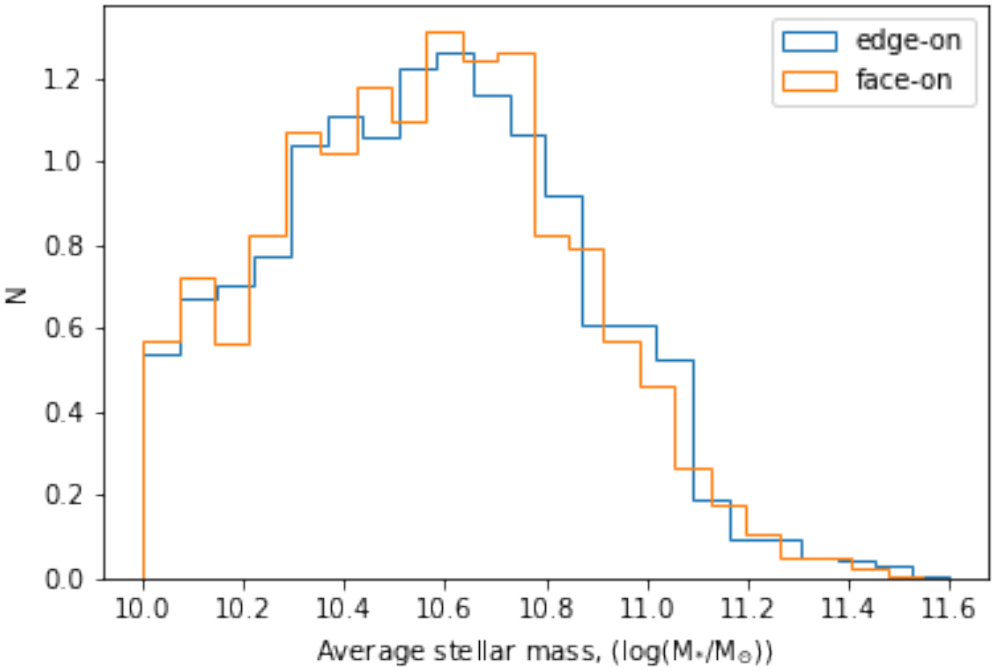


**Figure 3.5:** Average stellar mass of edge-on galaxies and face-on galaxies in the sample

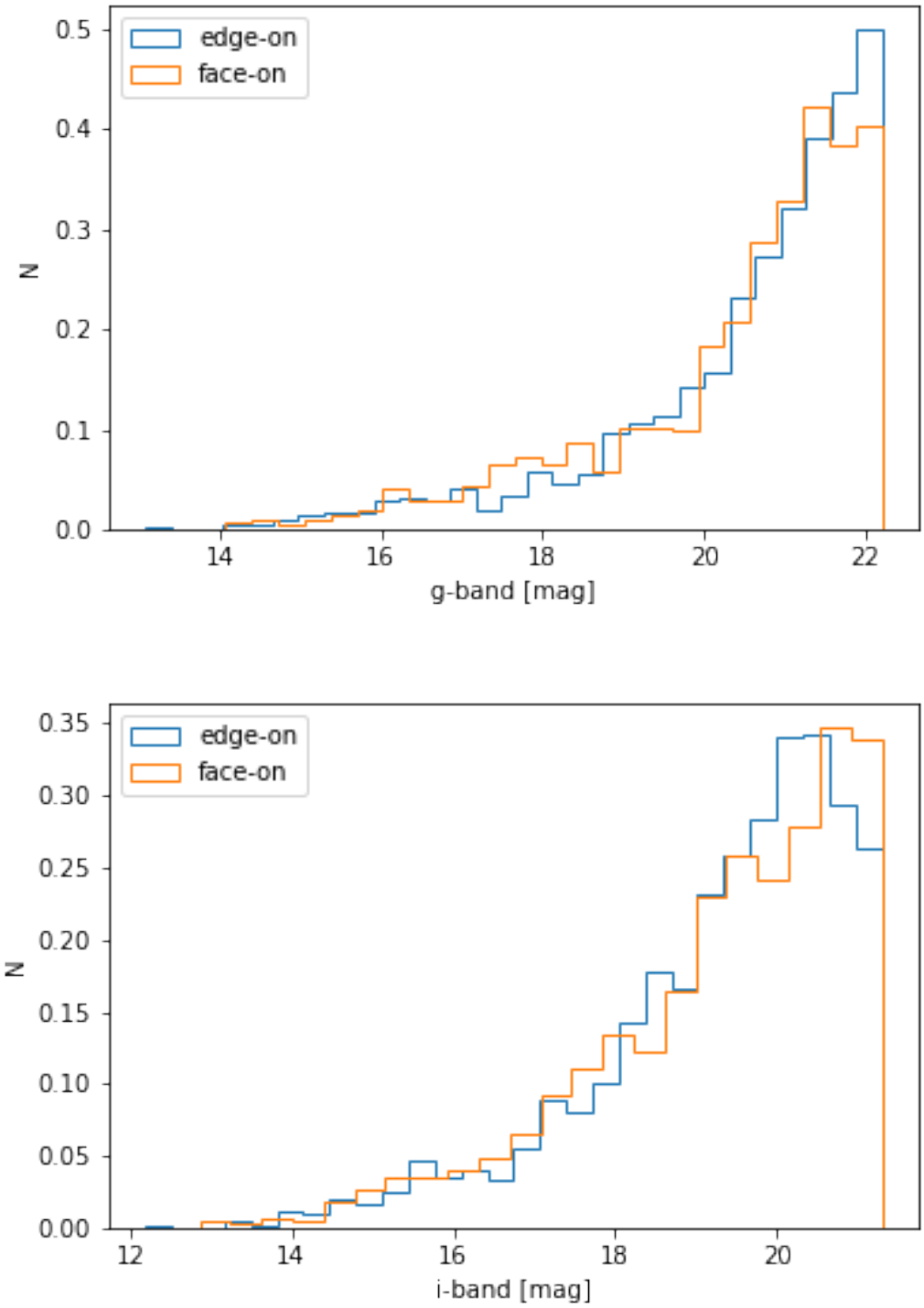


**Figure 3.6:** Magnitude of neighbour galaxies of edge-on and face-on galaxies in the sample in *g* and *i* bands

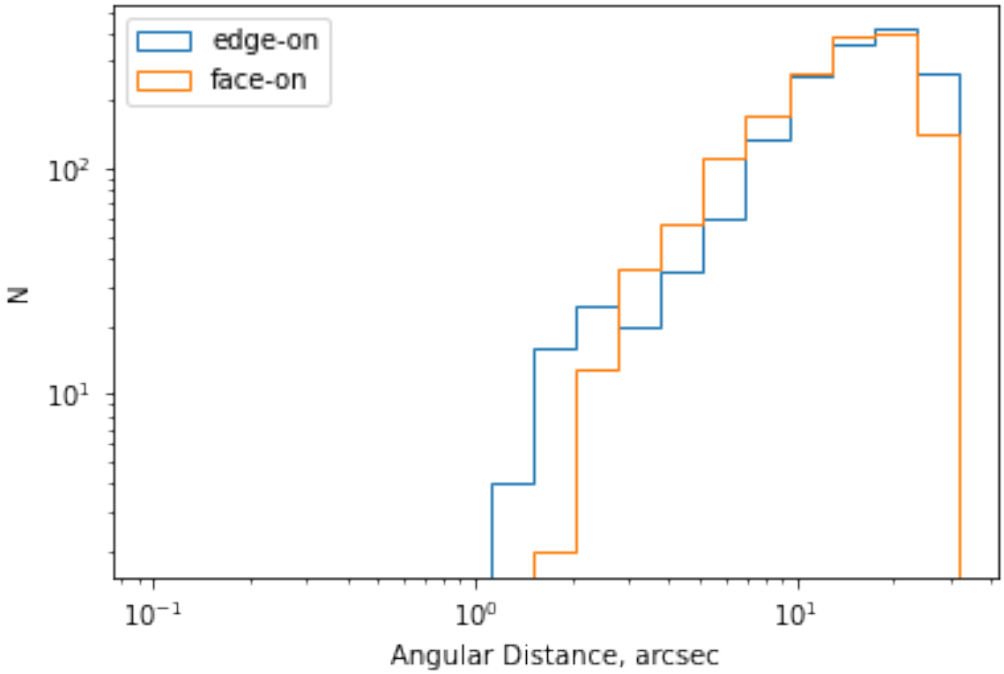


**Figure 3.7:** A plot of the distribution of the angular distance or separation of the neighbour galaxies from the edge-on and face-on galaxies in the sample.

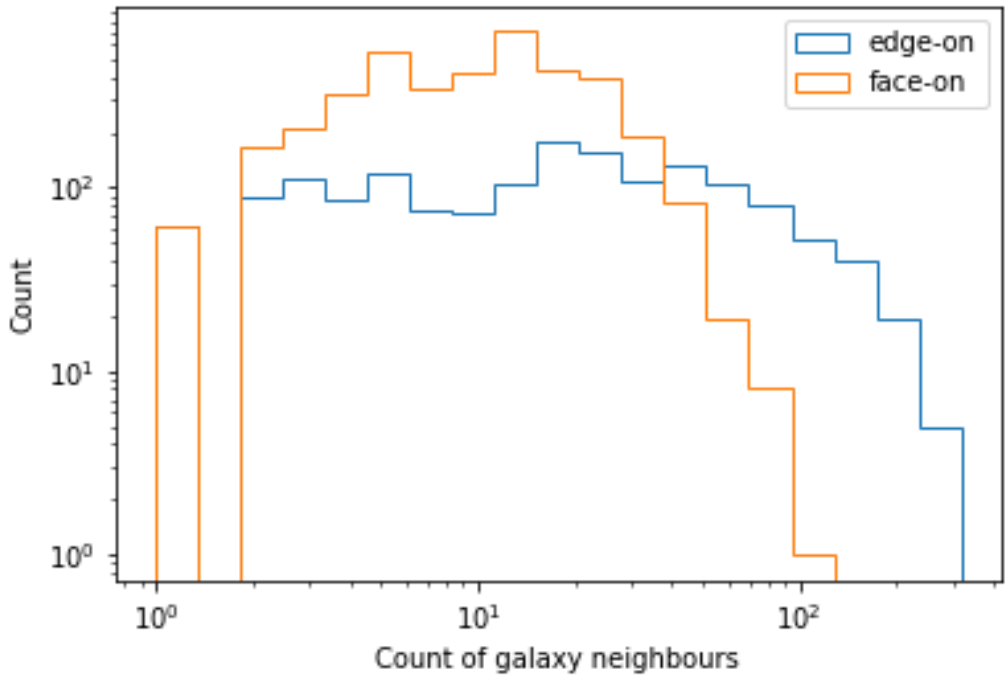


**Figure 3.8:** A comparison of the count of neighbour galaxies of edge-on galaxies in the sample and their corresponding face-on galaxies given the halo mass and average stellar mass controls. The mean count of neighbours for edge-on galaxies is higher than that of face-on galaxies

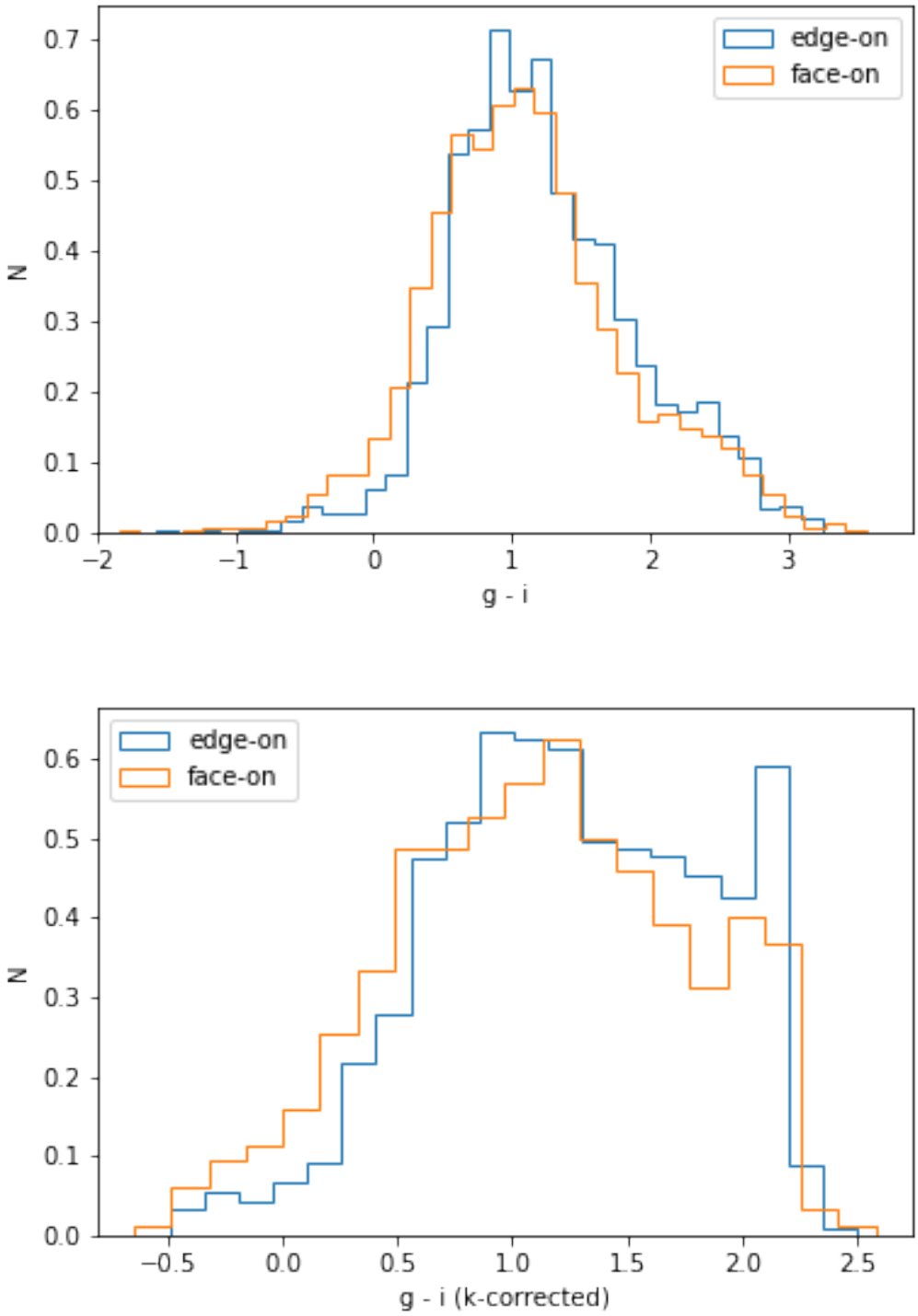


**Figure 3.9:** The $g - i$ of neighbour galaxies of edge-on and face-on galaxies in the sample

effect instead of a physical one since we controlled for parameters such as halo mass and average stellar mass. Therefore, the missing neighbours are present but might not be observable by SDSS due to face-on galaxies taking up more space in the sky than edge-on galaxies, and this could cause face-on galaxies to obscure more of their neighbour galaxies.

The result in the difference of neighbour galaxies being an observational bias can be further confirmed by Figure 3.6 where we plotted the magnitude of neighbour galaxies of edge-on and face-on galaxies in the sample in $g$ and $i$ bands. The figure shows that the face-on galaxies in the sample have more missing faint neighbour galaxies in the $g$-band than in the $i$-band which confirms that these faint neighbour galaxies are present but are more likely to go undetected due to obscuration by the face-on galaxy. Moreover, a plot of the angular distance distribution of the neighbours from the face-on and edge-on galaxies (Figure 3.7) in the matched sample, show more neighbour galaxies at the lower angular distances for edge-on galaxies than for face-on. This implies that neighbour galaxies that are closer to the face-on galaxies are more likely to be obscured relative to edge-on galaxies.

We also plotted the $g-i$ colour of the neighbours in order to identify if the environments of the galaxies are similar (Figure 3.9). Colour is relevant for neighbours because those near a massive galaxy could be influenced by its gravity, and this might lead to either additional star-formation or suppression of star-formation (Font et al., 2008; Skibba et al., 2009; Barsanti et al., 2018). If neighbours are red, it could indicate that there's some contamination or obscuration occurring, likely from light or dust respectively, due to the main galaxy absorbing and scattering the blue light from the neighbours, making them appear redder (Mathis, 1990). Even though star-formation and dust reddening are the two most physical factors, metallicity and age might also play a role in how red it is (Tremonti et al., 2004; Gallazzi et al., 2005). In Figure 3.9, a higher number indicates that the neighbour is redder, and conversely, a lower number indicates that the neighbour is bluer. Therefore, for face-on galaxies, there are a few more blue neighbours than there are for

edge-on galaxies. We performed a two-sample Kolmogorov-Smirnov (or ks) test which compared the two samples to see if they came from the same parent population. The ks test gives a $p$-value where if $p > a$ (where $a$ is usually set at 0.05 or 0.01) it means that there is no significant evidence that the distributions are drawn from different parent populations. The ks test performed here showed that the $p$-value for $g - i$ k-corrected is $2.53 \times 10^{-6}$ which implies that the parent samples are different. We could attribute this to the large dataset used in the analysis in addition to smearing and uncertainties associated with colour as the photometric data from SDSS (York et al., 2000).

### 3.3.1 Consequences for the unified theory of AGN

A galaxy's morphology is strongly linked to its environment and therefore it is crucial to account for it when conducting environmental analysis, such as investigating the number of neighbour galaxies. Our observations of an excess of neighbours around edge-on galaxies compared to face-on galaxies could affect such environmental analysis and one potential factor to consider is AGN.

AGN can be categorised as either radio-loud or radio-quiet AGN according to their radio emission and the presence of jets. Radio-loud AGN have very strong jets (Wilson & Colbert, 1995; Urry, 2003) where the relativistic jets interact with the interstellar matter producing synchrotron emission which causes radio emission (Blandford & Znajek, 1977). Radio-quiet AGN have very weak or no jets in the radio wavelength. Optical spectroscopy has shown that they can be further categorised as Type 1 AGN or Type 2 AGN based on observational properties such as the presence or absence of broad emission lines in their observed spectra. A Type 1 AGN exhibits broad permitted and semi-forbidden emission lines. The majority of Type 1 AGN of low to intermediate luminosity show high ionisation narrow emission lines including forbidden emission lines in their spectra and these are referred to as Seyfert 1 galaxies or QSOs (Netzer, 2015). Conversely, many high

luminosity Type 1 AGN show an absence of these narrow emission lines in their spectra. A Type 2 AGN show strong narrow emission lines in the NIR-optical-UV wavelengths and is the result of photoionization by a non-stellar source (Netzer, 2015; Hickox & Alexander, 2018).

Miller & Antonucci (1983) observed hidden broad emission lines in the polarised spectra of some Type 2 AGN. This indicates that Type 2 AGN can be further divided into two sub-groups: where one group contains hidden Type 1 sources with broad emission lines which are detectable in polarised light, and a second group which show narrow lines as expected but no detectable broad emission lines. The discovery of these hidden broad lines in the former sub-group suggested that the emission from Type 2 AGN passed through an optically thick material before it was observed and the unified model of AGN was proposed as a result of this discovery (Figure 3.10; Antonucci, 1993; Urry & Padovani, 1995).

In this model, the black hole and the accretion disk are surrounded by a geometrically and optically thick, roughly toroidal structure of dust and gas, referred to as a dusty torus. The torus was suggested to be responsible for scattering the light and is large enough to obscure the central engine in some directions. There are two other key regions in the unified model: the broad line region (BLR) and narrow line region (NLR) which are defined by the velocity widths of their observed emission lines (Netzer, 2015). The BLR is at a relatively close distance to the SMBH and is composed of dense, ionised gas with high velocities and exhibits broad emission lines in its spectra. The NLR extends to outside the torus and is composed of lower density gas, and shows permitted and forbidden narrow emission lines in its spectra. The torus's shape means that if an observer were to view an AGN face-on they would have an unobstructed view of the torus and central engine. The observed spectrum will include both broad and narrow emission lines and the AGN will be classed as a Type 1 AGN. On the other hand, if an AGN was viewed edge-on then the

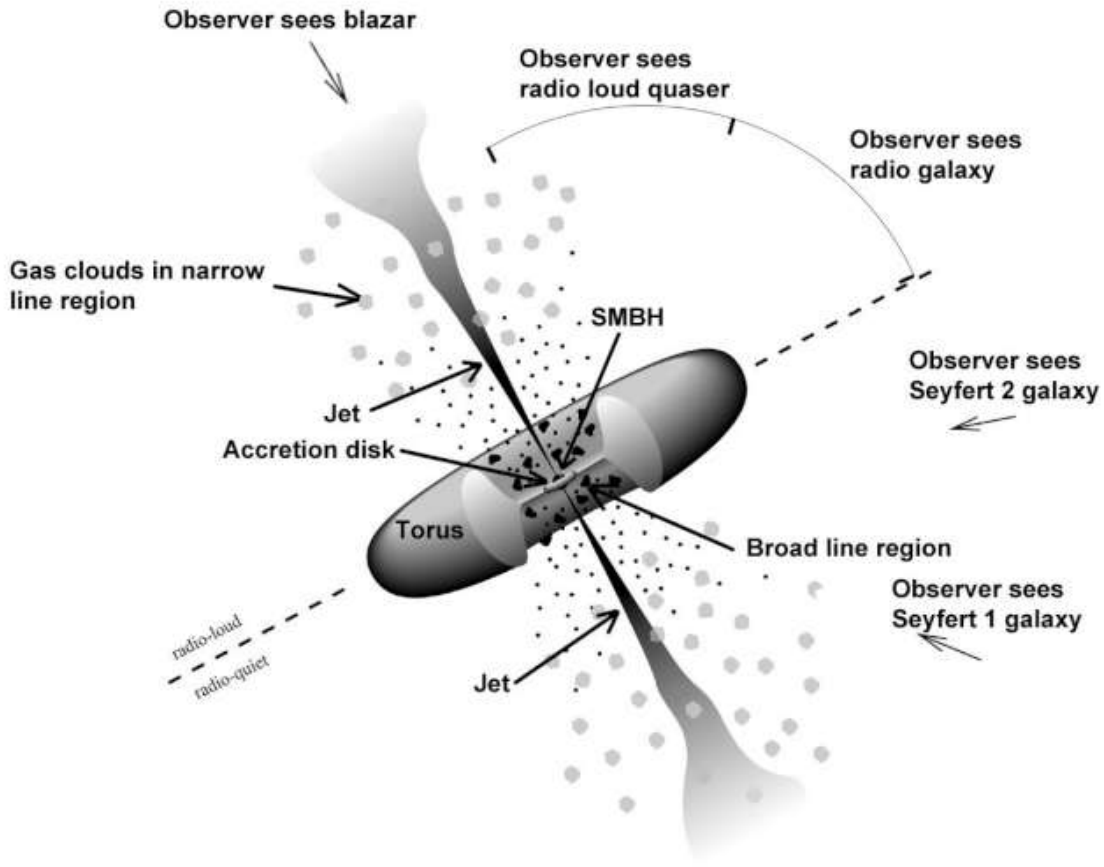


**Figure 3.10:** Diagram of an AGN as described in the unified model which shows the supermassive black hole (SMBH), accretion disk and broad line region (BLR) being obscured by a torus if an observer is looking at the AGN edge-on, however the narrow line region (NLR) and jets which extend to outside the torus can be still be detected in this case. Image Credit: Fermi Gamma-ray Space Telescope, obtained from https://fermi.gsfc.nasa.gov/science/eteu/agn

torus will obscure the central engine and the BLR. The NLR which extends further than the BLR and the torus would still be visible in this case. As such, only narrow emission lines will be visible in the object's spectra and there would be not be any indications of broad lines—hence the AGN would be classed as a Type 2 AGN (Antonucci, 1993; Heckman & Best, 2014). The torus model discussed here is a simplified one, but in a more realistic scenario the covering factor of a 'clumpy' torus will not be uniform and may vary between AGN (Elitzur, 2012).

In summary, the unified AGN model therefore states that AGN fall into two basic categories: those which are obscured by the dusty torus and those which are unobscured, and this depends on the observer's viewing angle of the AGN. According to this theory, both Type 1 and Type 2 AGN are the same type of galaxy and any differences in their observational properties can be attributed to the effect of their orientation relative to the observer's line-of-sight. Therefore, for a given luminosity there should not be any major or intrinsic differences between them and their surrounding environment. For example, a consequence of this would that we should expect to see a similar number of neighbour galaxies for both Type 1 and Type 2 AGN. However, observations have shown that Type 2 AGN are more likely to be in galaxy pairs than Type 1 AGN, with a projected separation of less than 100 kpc $h^{-1}$ (Dultzin-Hacyan et al., 1999; Koulouridis et al., 2006; Jiang et al., 2016). Villarroel & Korn (2014) also found this excess of Type 2 AGN pairs in AGN pairs at projected separations below 200 kpc. Conversely, other observations show this excess of Type 2 AGN in the fractions of AGN in pairs only in separations smaller than 20 kpc $h^{-1}$ and 500 km $s^{-1}$ (Gordon et al., 2016). In this thesis, we have shown that more neighbours are observed for edge-on galaxies than for face-on galaxies once controlling for halo mass and stellar mass, and this observation bias could potentially account for the observed excess of Type 2 AGN in pairs.

This can be tested by analysing whether or not Type 2 AGN are more frequently

associated with edge-on galaxies than face-on galaxies. Keel (1980) noted a deficit of Type 1 AGN in edge-on galaxies which was further corroborated by Maiolino & Rieke (1995) who suggested that Type 1 galaxies may potentially be hidden by gas and dust by the host edge-on galaxies. Schmitt et al. (2001) conducted statistical tests on Type 1 and Type 2 galaxies, where the sample was selected based on mainly isotropic properties such as their colour and far-infrared flux, and found that there were fewer Type 1 AGN in edge-on galaxies. However, there were no statistically significant differences when comparing the morphological types of the host galaxies. We have conducted a preliminary test to see if these results are consistent when separating the galaxies in the sample as Type 1 or Type 2 AGN. Using the 'Subclass' criteria in the MPA-JHU catalogue, we separated the neighbours into 'Broadline' or 'AGN' which corresponds to Type 1 and Type 2 galaxies respectively, and conducted the same analysis as outlined in Section 3.2.

Separating the sample by Type 1 and Type 2 AGN yielded 296 rows for edge-on galaxies and 3142 rows for face-on galaxies for Type 1, and 109 rows for edge-on galaxies and 1623 rows for face-on galaxies for Type 2. Controlling for halo mass and stellar mass generated a sample of 291 neighbours for Type 1 AGN and 106 neighbours for Type 2 AGN. For Type 1 AGN, the mean count and median of neighbours for edge-on galaxies were 30.91 and 18.00 with lower quartile of 6.00 and upper quartile of 42.00, and for face-on galaxies the mean count and median were 12.64 and 10.00 with lower quartile of 6.00 and upper quartile of 16.00. For Type 2 AGN, the mean count and median for edge-on galaxies were 24.50 and 10.00 with lower quartile of 3.00 and upper quartile of 21.75, and for face-on galaxies the mean count and median were 12.25 and 8.50 with lower quartile of 4.00 and upper quartile of 15.25. Despite the sample size for this preliminary test being much smaller than that used in the bulk of the thesis, the results were consistent and showed an excess of neighbours for edge-on galaxies than for face-on galaxies in both Type 1 and Type 2 AGN (Figure 3.11).

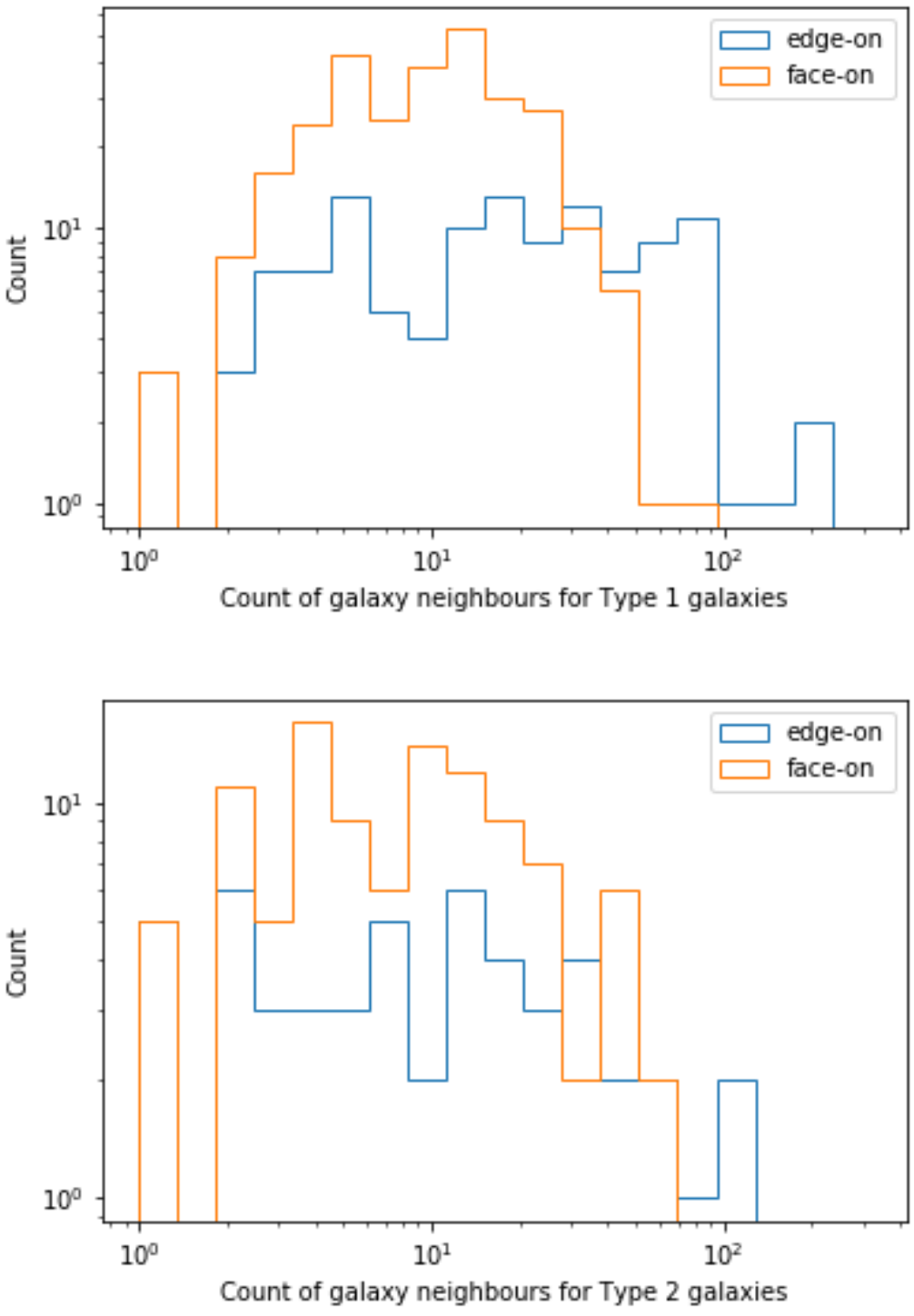


**Figure 3.11:** A comparison of the count of neighbour galaxies for Type 1 and Type 2 galaxies

# 4. Conclusions

In this thesis, we compared the number of neighbours for edge-on and face-on galaxies using data from SDSS, GZ2 and Yang et al. (2007) catalogue in order to determine if galaxy orientation impacts the number of neighbours detected. The results showed that the number of neighbours for edge-on galaxies was higher than that of face-on galaxies after controlling for parameters such as halo mass and average stellar mass. Having controlled against potential physical drivers of this effect, our results are consistent with this being an observational bias instead of a physical effect. This means that the face-on galaxies obscure the detection of more nearby neighbour galaxies. Therefore, we have quantified the observational excess or bias of neighbours around edge-on galaxies than face-on galaxies, and this bias needs to be accounted for in future research on neighbour galaxies and related environmental analysis.

This result might also have consequences for the unified theory of AGN. According to this model, the difference in the properties of Type 1 and Type 2 AGN only arise due to their orientation relative to the observer and analysis of their environments should reflect this. However, many studies have observed that Type 2 AGN have more neighbours than Type 1 AGN without accounting for morphology (Dultzin-Hacyan et al., 1999; Koulouridis et al., 2006; Jiang et al., 2016; Villarroel & Korn, 2014; Gordon et al., 2016). A preliminary test showed that this observational bias was also present when we separated the sample by Type 1 and Type 2 AGN. Potential future works would test if Type 2 AGN are more frequently associated with edge-on galaxies than face-on since observations show that there is a deficiency of Type 1 AGN in edge-on galaxies (Keel, 1980; Maiolino & Rieke, 1995; Schmitt et al., 2001). The next stage would then be to determine if this can explain the

excess of neighbours observed around Type 2 AGN relative to Type 1 AGN.

# Bibliography


Abazajian K. N., et al., 2009, The Astrophysical Journal Supplement Series, 182, 543–558

Abell G. O., 1958, ApJS, 3, 211

Alonso M. S., Lambas D. G., Tissera P., Coldwell G., 2007, Monthly Notices of the Royal Astronomical Society, 375, 1017

Antonucci R., 1993, ARA&A, 31, 473

Bamford S. P., et al., 2009, Monthly Notices of the Royal Astronomical Society, 393, 1324–1352

Barsanti S., et al., 2018, The Astrophysical Journal, 857, 71

Belfiore F., et al., 2016, Monthly Notices of the Royal Astronomical Society, 461, 3111–3134

Bell E. F., McIntosh D. H., Katz N., Weinberg M. D., 2003, ApJS, 149, 289

Blandford R. D., Znajek R. L., 1977, MNRAS, 179, 433

Blandford R., Meier D., Readhead A., 2019, Annual Review of Astronomy and Astrophysics, 57, 467–509

Blanton M. R., et al., 2005, The Astronomical Journal, 129, 2562–2578

Blumenthal G. R., Faber S. M., Primack J. R., Rees M. J., 1984, Nature, 311, 517

Bower R. G., Kodama T., Terlevich A., 1998, Monthly Notices of the Royal Astronomical Society, 299, 1193–1208

Brinchmann J., Charlot S., White S. D. M., Tremonti C., Kauffmann G., Heckman T., Brinkmann J., 2004, MNRAS, 351, 1151

Cole S., Lacey C. G., Baugh C. M., Frenk C. S., 2000, MNRAS, 319, 168

Conselice C. J., 2014, Annual Review of Astronomy and Astrophysics, 52, 291–337

Croton D. J., et al., 2006, Monthly Notices of the Royal Astronomical Society, 365, 11–28

Davis M., Efstathiou G., Frenk C. S., White S. D. M., 1985, ApJ, 292, 371

De Lucia G., Springel V., White S. D. M., Croton D., Kauffmann G., 2006, MNRAS, 366, 499

Dressler A., 1980, ApJ, 236, 351

Dultzin-Hacyan D., Krongold Y., Fuentes-Guridi I., Marziani P., 1999, The Astrophysical Journal, 513, L111

Eddington A. S., 1924, Monthly Notices of the Royal Astronomical Society, 84, 308

Elitzur M., 2012, The Astrophysical Journal, 747, L33

Ellison S. L., Patton D. R., Mendel J. T., Scudder J. M., 2011, Monthly Notices of the Royal Astronomical Society, 418, 2043–2053

Ellison S. L., Patton D. R., Hickox R. C., 2015, Monthly Notices of the Royal Astronomical Society: Letters, 451, L35–L39

Faber S. M., Jackson R. E., 1976, ApJ, 204, 668

Fabian A., 2012, Annual Review of Astronomy and Astrophysics, 50, 455–489

Ferrarese L., Merritt D., 2000, The Astrophysical Journal, 539, L9–L12

Fliri J., Trujillo I., 2015, Monthly Notices of the Royal Astronomical Society, 456, 1359–1373

Font A. S., et al., 2008, Monthly Notices of the Royal Astronomical Society, 389, 1619–1629

Fukugita M., Ichikawa T., Gunn J. E., Doi M., Shimasaku K., Schneider D. P., 1996, AJ, 111, 1748

Gallazzi A., Charlot S., Brinchmann J., White S. D. M., Tremonti C. A., 2005, Monthly Notices of the Royal Astronomical Society, 362, 41–58

Gawiser E., Silk J., 2000, Physics articles, 333-334, 245–267

Gebhardt K., et al., 2000, The Astrophysical Journal, 539, L13

Gordon Y. A., et al., 2016, Monthly Notices of the Royal Astronomical Society, 465, 2671–2686

Gordon Y. A., Pimbblet K. A., Owers M. S., 2018, Research Notes of the American Astronomical Society, 2, 132

Gordon Y. A., et al., 2019, The Astrophysical Journal, 878, 88

Gunn J. E., et al., 1998, The Astronomical Journal, 116, 3040

Heckman T. M., Best P. N., 2014, Annual Review of Astronomy and Astrophysics, 52, 589–660

Hickox R. C., Alexander D. M., 2018, Annual Review of Astronomy and Astrophysics, 56, 625–671

Hinshaw G., et al., 2013, The Astrophysical Journal Supplement Series, 208, 19

Ho L. C., 2008, Annual Review of Astronomy and Astrophysics, 46, 475–539

Houghton R. C. W., 2015, Monthly Notices of the Royal Astronomical Society, 451, 3427

Hubble E. P., 1926, ApJ, 64, 321

Jiang N., Wang H., Mo H., Dong X.-B., Wang T., Zhou H., 2016, The Astrophysical Journal, 832, 111

Kauffmann G., et al., 2003, Monthly Notices of the Royal Astronomical Society, 341, 33–53

Keel W. C., 1980, AJ, 85, 198

King A., Pounds K., 2015, Annual Review of Astronomy and Astrophysics, 53, 115–154

Kormendy J., 2013, Secular Evolution in Disk Galaxies

Kormendy J., Ho L. C., 2013, Annual Review of Astronomy and Astrophysics, 51, 511–653

Koulouridis E., Plionis M., Chavushyan V., Dultzin-Hacyan D., Krongold Y., Goudis C., 2006, The Astrophysical Journal, 639, 37–45

Lacey C., Cole S., 1994, Monthly Notices of the Royal Astronomical Society, 271, 676–692

Lahav O., Lilje P. B., Primack J. R., Rees M. J., 1991, MNRAS, 251, 128

Lange J. U., van den Bosch F. C., Hearin A., Campbell D., Zentner A. R., Villarreal A., Mao Y.-Y., 2017, Monthly Notices of the Royal Astronomical Society, 473, 2830–2851

Lintott C. J., et al., 2008, Monthly Notices of the Royal Astronomical Society, 389, 1179–1189

Lintott C., et al., 2010, Monthly Notices of the Royal Astronomical Society, 410, 166–178

Magorrian J., et al., 1998, AJ, 115, 2285

Maiolino R., Rieke G. H., 1995, ApJ, 454, 95

Martig M., Bournaud F., Croton D. J., Dekel A., Teyssier R., 2012, The Astrophysical Journal, 756, 26

Martini P., Kelson D. D., Kim E., Mulchaey J. S., Athey A. A., 2006, The Astrophysical Journal, 644, 116–132

Masters K. L., et al., 2010, Monthly Notices of the Royal Astronomical Society

Mathis J. S., 1990, ARA&A, 28, 37

Merritt D., Ferrarese L., 2001, Monthly Notices of the Royal Astronomical Society, 320, L30–L34

Miller J. S., Antonucci R. R. J., 1983, ApJL, 271, L7

Moore B., Katz N., Lake G., Dressler A., Oemler A., 1996, Nature, 379, 613–616

Mutch S. J., Croton D. J., Poole G. B., 2013, Monthly Notices of the Royal Astronomical Society, 435, 2445–2459

Navarro J. F., Frenk C. S., White S. D. M., 1996, The Astrophysical Journal, 462, 563

Netzer H., 2015, Annual Review of Astronomy and Astrophysics, 53, 365–408

Pearson W. J., et al., 2019, Astronomy & Astrophysics, 631, A51

Peebles P. J. E., 1965, ApJ, 142, 1317

Peebles P. J. E., 1980, The large-scale structure of the universe

Penzias A. A., Wilson R. W., 1965, ApJ, 142, 419

Perlmutter S., et al., 1999, The Astrophysical Journal, 517, 565–586

Planck Collaboration et al., 2016, A&A, 594, A1

Postman M., Geller M. J., 1984, ApJ, 281, 95

Riess A. G., et al., 1998, The Astronomical Journal, 116, 1009–1038

Russell H. N., 1914, Popular Astronomy, 22, 275

Salim S., et al., 2007, The Astrophysical Journal Supplement Series, 173, 267–292

Scannapieco C., Tissera P. B., White S. D. M., Springel V., 2008, Monthly Notices of the Royal Astronomical Society, 389, 1137–1149

Schawinski K., et al., 2014, Monthly Notices of the Royal Astronomical Society, 440, 889–907

Schmidt B. P., et al., 1998, The Astrophysical Journal, 507, 46–63

Schmitt H. R., Antonucci R. R. J., Ulvestad J. S., Kinney A. L., Clarke C. J., Pringle J. E., 2001, The Astrophysical Journal, 555, 663–672

Seyfert C. K., 1943, ApJ, 97, 28

Skibba R. A., 2009, Monthly Notices of the Royal Astronomical Society, 392, 1467–1474

Skibba R. A., et al., 2009, MNRAS, 399, 966

Springel V., et al., 2005, Nature, 435, 629

Strateva I., et al., 2001, The Astronomical Journal, 122, 1861

Tonnesen S., Bryan G. L., 2009, The Astrophysical Journal, 694, 789–804

Toomre A., Toomre J., 1972, ApJ, 178, 623

Tremonti C. A., et al., 2004, The Astrophysical Journal, 613, 898–913

Urry M., 2003, Astronomical Society of the Pacific Conference Series, 290, 3

Urry C. M., Padovani P., 1995, Publications of the Astronomical Society of the Pacific, 107, 803

Van Den Bosch F. C., Aquino D., Yang X., Mo H. J., Pasquali A., McIntosh D. H., Weinmann S. M., Kang X., 2008, Monthly Notices of the Royal Astronomical Society, 387, 79

Villarroel B., Korn A. J., 2014, Nature Physics, 10, 417–420

Visvanathan N., Sandage A., 1977, ApJ, 216, 214

Wang E., et al., 2018, The Astrophysical Journal, 860, 102

Weinmann S. M., Kauffmann G., van den Bosch F. C., Pasquali A., McIntosh D. H., Mo H., Yang X., Guo Y., 2009, Monthly Notices of the Royal Astronomical Society, 394, 1213–1228

White M., 2001, Astronomy & Astrophysics, 367, 27–32

White S. D. M., Rees M. J., 1978, MNRAS, 183, 341

Willett K. W., et al., 2013, Monthly Notices of the Royal Astronomical Society, 435, 2835–2860

Wilson A. S., Colbert E. J. M., 1995, The Astrophysical Journal, 438, 62

Woo J., Carollo C. M., Faber S. M., Dekel A., Tacchella S., 2016, Monthly Notices of the Royal Astronomical Society, 464, 1077–1094

Woolfson M. M., 1993, , 34, 1

Yang X., Mo H. J., van den Bosch F. C., Pasquali A., Li C., Barden M., 2007, The Astrophysical Journal, 671, 153–170

Yoon J. H., Schawinski K., Sheen Y.-K., Ree C. H., Yi S. K., 2008, The Astrophysical Journal Supplement Series, 176, 414

York D. G., et al., 2000, The Astronomical Journal, 120, 1579–1587

Zel'Dovich Y. B., 1970, A&A, 500, 13

Zwicky F., 1933, Helvetica Physica Acta, 6, 110